Supercooling super-droplets: on particle-based modelling of immersion freezing

S. Arabas[1], J.H. Curtis[2], I. Silber[3], A. Fridlind[4], D.A Knopf[5], M. West[2] & N. Riemer[2]

1: JAGIELLONIAN UNIVERSITY uj.edu.pl
2: atmos.illinois.edu
3: met.psu.edu
4: giss.nasa.gov
5: stonybrook.edu

funding: ASR Atmospheric System Research

virtual Mathematics and Atmospheric Physics Seminar @ UMainz, July 6 2022

aerosol-cloud interactions: a conceptual picture

aerosol-cloud interactions: a conceptual picture

background image: `vitsly.ru` / Hokusai

aerosol-cloud interactions: a conceptual picture

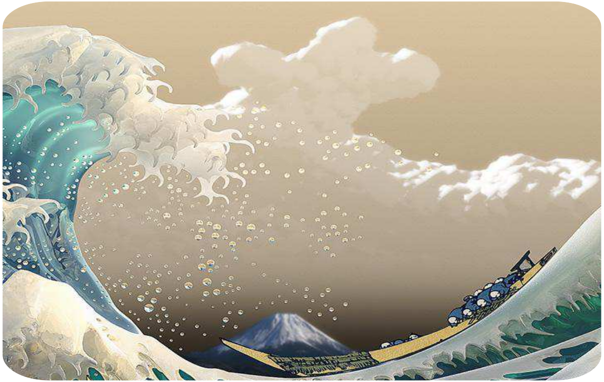

background image: `vitsly.ru` / Hokusai

aerosol-cloud interactions: a conceptual picture

- aerosol particles of natural and anthropogenic origin act as condensation/crystallisation nuclei

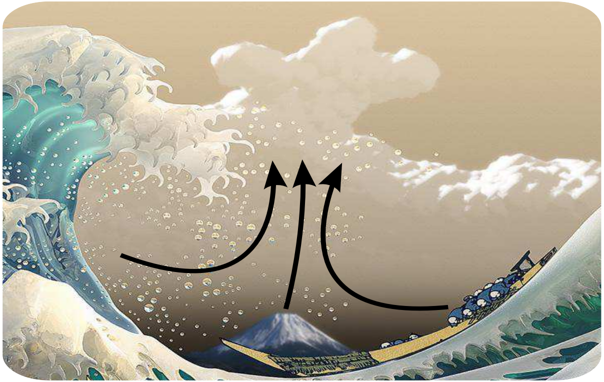

background image: vitsly.ru / Hokusai

aerosol-cloud interactions: a conceptual picture

- aerosol particles of natural
  and anthropogenic origin
  act as condensation/crystallisation nuclei
- droplets and ice particles grow through
  vapour condensation and deposition...

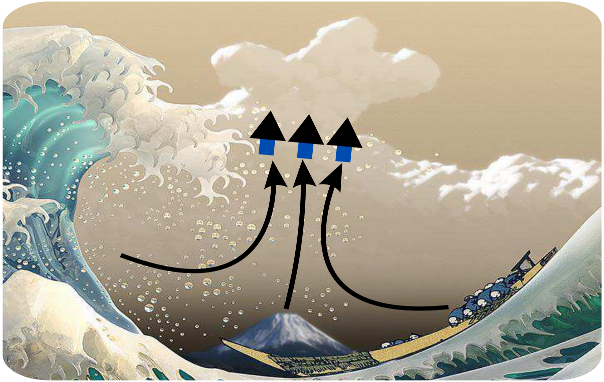

background image: vitsly.ru / Hokusai

aerosol-cloud interactions: a conceptual picture

- aerosol particles of natural and anthropogenic origin act as condensation/crystallisation nuclei
- droplets and ice particles grow through vapour condensation and deposition...
- ... and collisions-coalescence/aggregation

background image: `vitsly.ru` / Hokusai

aerosol-cloud interactions: a conceptual picture

- aerosol particles of natural and anthropogenic origin act as condensation/crystallisation nuclei
- droplets and ice particles grow through vapour condensation and deposition…
- … and collisions-coalescence/aggregation
- aqueous chemical reactions alter droplet composition

background image: vitsly.ru / Hokusai

aerosol-cloud interactions: a conceptual picture

- aerosol particles of natural and anthropogenic origin act as condensation/crystallisation nuclei
- droplets and ice particles grow through vapour condensation and deposition...
- ... and collisions-coalescence/aggregation
- aqueous chemical reactions alter droplet composition
- water and ice precipitates (possibly breaking up into smaller particles) washing out sub-cloud aerosol

background image: vitsly.ru / Hokusai

aerosol-cloud interactions: a conceptual picture

- aerosol particles of natural
  and anthropogenic origin
  act as condensation/crystallisation nuclei
- droplets and ice particles grow through
  vapour condensation and deposition...
- ... and collisions-coalescence/aggregation
- aqueous chemical reactions alter
  droplet composition
- water and ice precipitates
  (possibly breaking up into smaller particles)
  washing out sub-cloud aerosol
- particles evaporating before reaching surface
  (with potentially altered size/composition)
  contribute to ambient aerosol

background image: vitsly.ru / Hokusai

super-particles as a probabilistic alternative to bulk or bin μ-physics

JAMES | Journal of Advances in Modeling Earth Systems

COMMISSIONED MANUSCRIPT

10.1029/2019MS001689

Key Points:

- Microphysics is an important component of weather and climate models, but its representation in current models is highly uncertain

Confronting the Challenge of Modeling Cloud and Precipitation Microphysics

Hugh Morrison[1], Marcus van Lier-Walqui[2], Ann M. Fridlind[3], Wojciech W. Grabowski[1], Jerry Y. Harrington[4], Corinna Hoose[5], Alexei Korolev[6], Matthew R. Kumjian[4], Jason A. Milbrandt[7], Hanna Pawlowska[8], Derek J. Posselt[9], Olivier P. Prat[10], Karly J. Reimel[4], Shin-Ichiro Shima[11], Bastiaan van Diedenhoven[2], and Lulin Xue[1]

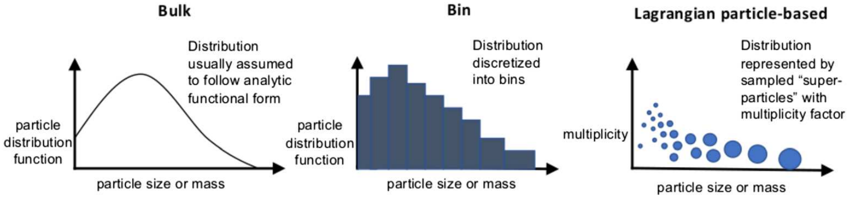

Figure 3. Representation of cloud and precipitation particle distributions in the three main types of microphysics

super-particles as a probabilistic alternative to bulk or bin μ-physics

JAMES | Journal of Advances in Modeling Earth Systems

COMMISSIONED MANUSCRIPT
10.1029/2019MS001689

Key Points:
- Microphysics is an important component of weather and climate models, but its representation in current models is highly uncertain

Confronting the Challenge of Modeling Cloud and Precipitation Microphysics

Hugh Morrison[1], Marcus van Lier-Walqui[2], Ann M. Fridlind[3], Wojciech W. Grabowski[1], Jerry Y. Harrington[4], Corinna Hoose[5], Alexei Korolev[6], Matthew R. Kumjian[4], Jason A. Milbrandt[7], Hanna Pawlowska[8], Derek J. Posselt[9], Olivier P. Prat[10], Karly J. Reimel[4], Shin-Ichiro Shima[11], Bastiaan van Diedenhoven[2], and Lulin Xue[1]

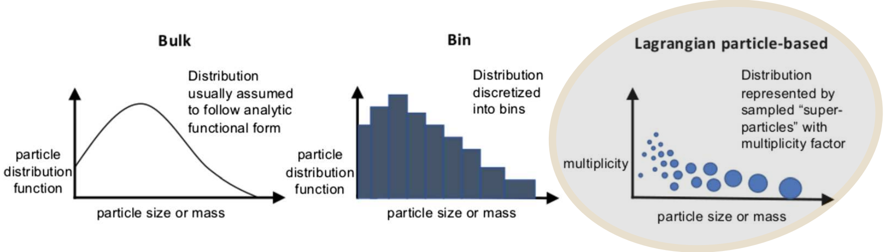

Figure 3. Representation of cloud and precipitation particle distributions in the three main types of microphysics

modelling cloud μ-physics: Eulerian vs. Lagrangian approaches

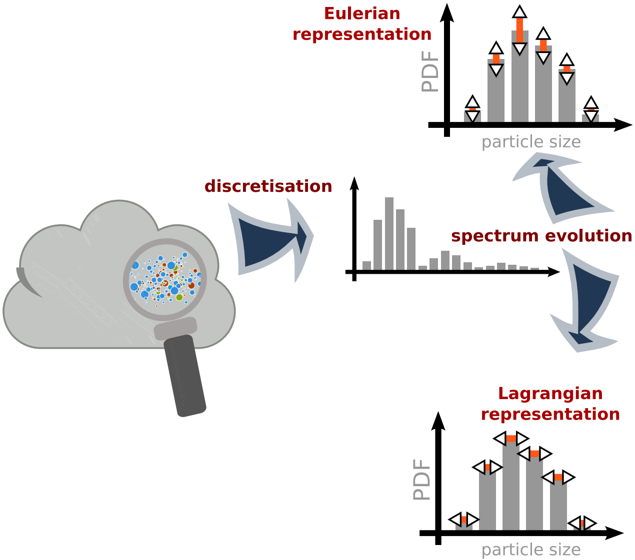

modelling cloud μ-physics: Eulerian vs. Lagrangian approaches

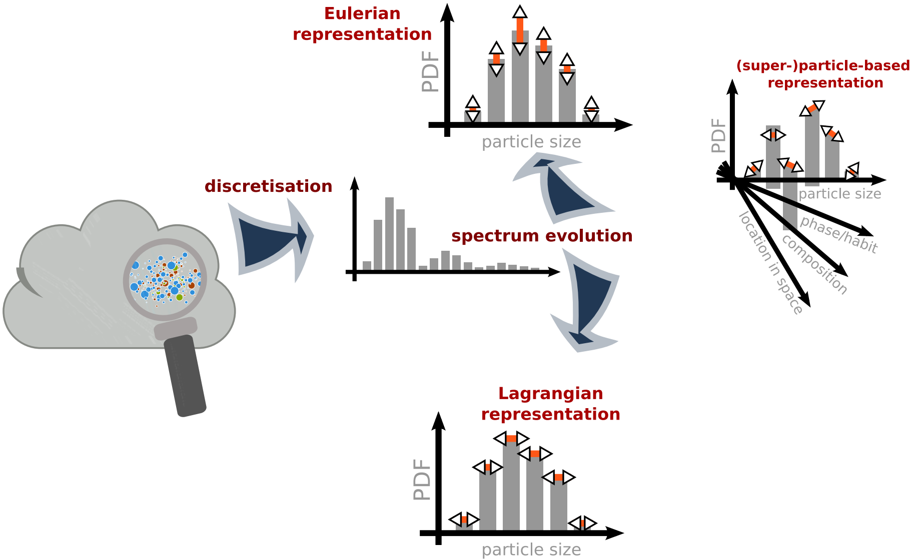

modelling cloud μ-physics: Eulerian vs. Lagrangian approaches

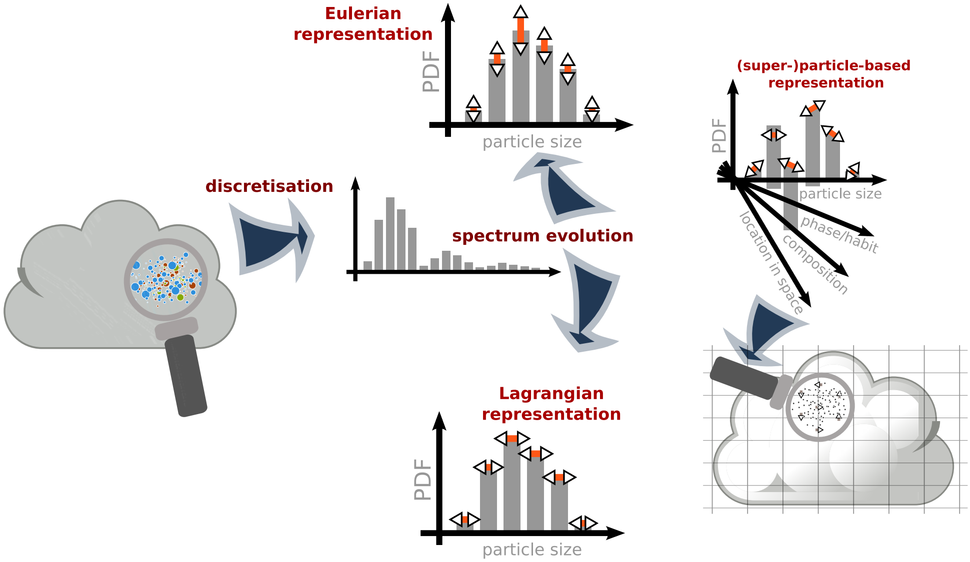

modelling cloud μ-physics: Eulerian vs. Lagrangian approaches

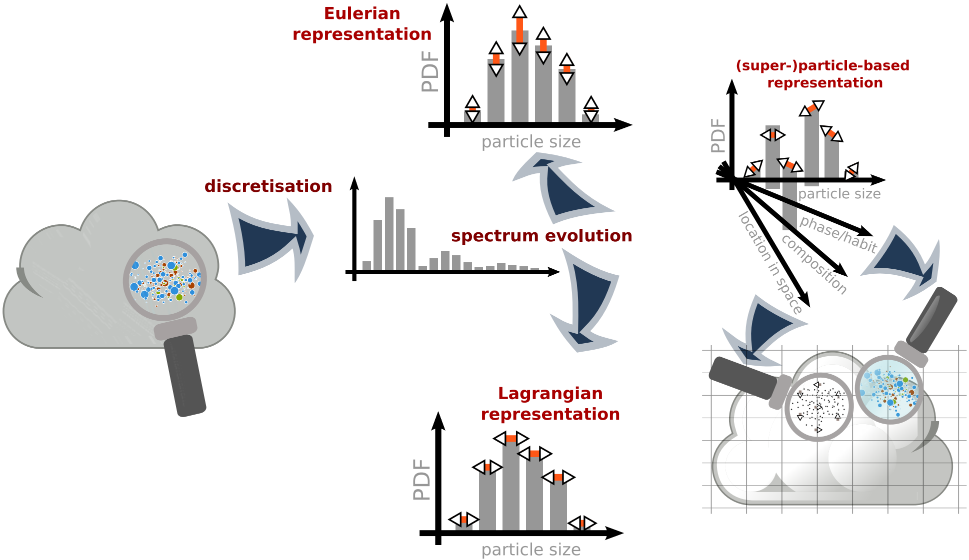

aerosol-cloud interactions: a conceptual picture

- aerosol particles of natural and anthropogenic origin act as condensation/crystallisation nuclei
- droplets and ice particles grow through vapour condensation and deposition…
- … and collisions-coalescence/aggregation
- aqueous chemical reactions alter droplet composition
- water and ice precipitates (possibly breaking up into smaller particles) washing out sub-cloud aerosol
- particles evaporating before reaching surface (with potentially altered size/composition) contribute to ambient aerosol

background image: vitsly.ru / Hokusai

aerosol-cloud interactions: a conceptual picture

- aerosol particles of natural and anthropogenic origin act as condensation/crystallisation nuclei
- droplets and ice particles grow through vapour condensation and deposition...
- ... and collisions-coalescence/aggregation
- aqueous chemical reactions alter droplet composition
- water and ice precipitates (possibly breaking up into smaller particles) washing out sub-cloud aerosol
- particles evaporating before reaching surface (with potentially altered size/composition) contribute to ambient aerosol

two-way interactions:
- aerosol characteristics influence cloud microstructure
- cloud processes influence aerosol size and composition

background image: vitsly.ru / Hokusai

super-particles as a probabilistic alternative to bulk or bin μ-physics

JAMES | Journal of Advances in Modeling Earth Systems

COMMISSIONED MANUSCRIPT
10.1029/2019MS001689

Key Points:

- Microphysics is an important component of weather and climate models, but its representation in current models is highly uncertain

Confronting the Challenge of Modeling Cloud and Precipitation Microphysics

Hugh Morrison[1], Marcus van Lier-Walqui[2], Ann M. Fridlind[3], Wojciech W. Grabowski[1], Jerry Y. Harrington[4], Corinna Hoose[5], Alexei Korolev[6], Matthew R. Kumjian[4], Jason A. Milbrandt[7], Hanna Pawlowska[8], Derek J. Posselt[9], Olivier P. Prat[10], Karly J. Reimel[4], Shin-Ichiro Shima[11], Bastiaan van Diedenhoven[2], and Lulin Xue[1]

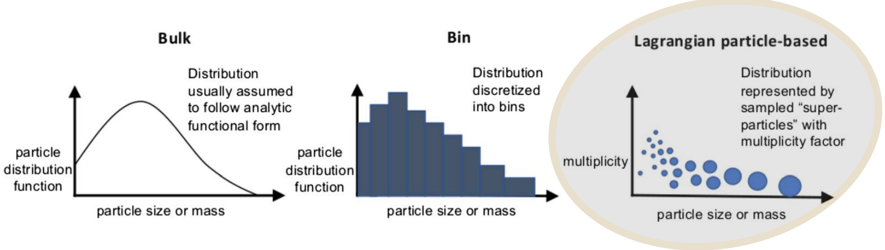

Figure 3. Representation of cloud and precipitation particle distributions in the three main types of microphysics

Shima et al. '20 particle-based mixed-phase μ-physics

Shima, Sato, Hashimoto & Misumi 2020 (GMD):
Predicting the morphology of ice particles in deep convection using the super-droplet method

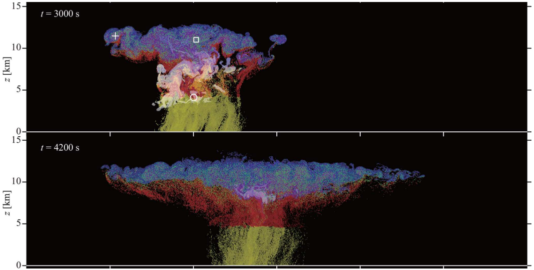

Figure 1. Typical realization of CTRL cloud spatial structures at $t = 2040$, 2460, 3000, 4200, and 5400 s. The mixing ratio of cloud water, rainwater, cloud ice, graupel, and snow aggregates are plotted in fading white, yellow, blue, red, and green, respectively. The symbols indicate examples of unrealistic predicted ice particles (Sects. 7.3 and 9.1). See also Movie 1 in the video supplement.

Shima et al. ’20 particle-based mixed-phase μ-physics

Shima, Sato, Hashimoto & Misumi 2020 (GMD):
Predicting the morphology of ice particles in deep convection using the super-droplet method

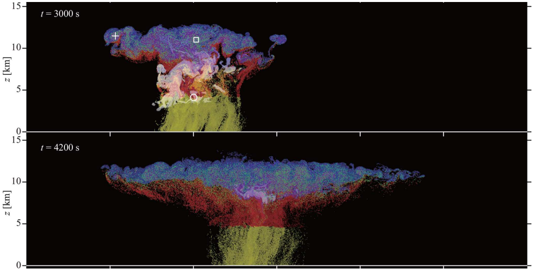

Figure 1. Typical realization of CTRL cloud spatial structures at $t = 2040$, 2460, 3000, 4200, and 5400 s. The mixing ratio of cloud water, rainwater, cloud ice, graupel, and snow aggregates are plotted in fading white, yellow, blue, red, and green, respectively. The symbols indicate examples of unrealistic predicted ice particles (Sects. 7.3 and 9.1). See also Movie 1 in the video supplement.

- Eulerian component: momentum, heat, moisture budget

Shima, Sato, Hashimoto & Misumi 2020 (GMD):

Predicting the morphology of ice particles in deep convection using the super-droplet method

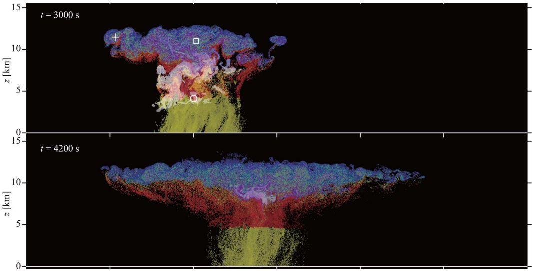

Figure 1. Typical realization of CTRL cloud spatial structures at $t = 2040$, 2460, 3000, 4200, and 5400 s. The mixing ratio of cloud water, rainwater, cloud ice, graupel, and snow aggregates are plotted in fading white, yellow, blue, red, and green, respectively. The symbols indicate examples of unrealistic predicted ice particles (Sects. 7.3 and 9.1). See also Movie 1 in the video supplement.

- Eulerian component: momentum, heat, moisture budget
- Lagrangian component: super particles representing aerosol, water droplets, ice particles (porous spheroids)

Shima et al. '20 particle-based mixed-phase μ-physics

Shima, Sato, Hashimoto & Misumi 2020 (GMD):

Predicting the morphology of ice particles in deep convection using the super-droplet method

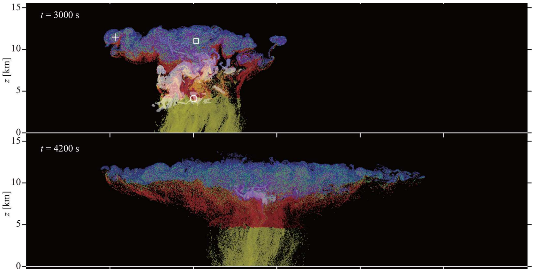

Figure 1. Typical realization of CTRL cloud spatial structures at $t = 2040$, 2460, 3000, 4200, and 5400 s. The mixing ratio of cloud water, rainwater, cloud ice, graupel, and snow aggregates are plotted in fading white, yellow, blue, red, and green, respectively. The symbols indicate examples of unrealistic predicted ice particles (Sects. 7.3 and 9.1). See also Movie 1 in the video supplement.

- Eulerian component: momentum, heat, moisture budget
- Lagrangian component: super particles representing aerosol, water droplets, ice particles (porous spheroids)
- particle-resolved processes:
  — advection and sedimentation
  — homogeneous and immersion freezing (singular)
  — melting
  — condensation and evaporation (incl. CCN [de]activation)
  — deposition and sublimation
  — collisions (coalescence, riming, aggregation, washout)

Shima et al. '20 particle-based mixed-phase μ-physics

Shima, Sato, Hashimoto & Misumi 2020 (GMD):

Predicting the morphology of ice particles in deep convection using the super-droplet method

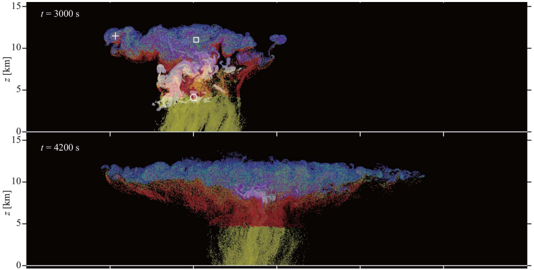

Figure 1. Typical realization of CTRL cloud spatial structures at $t = 2040$, 2460, 3000, 4200, and 5400 s. The mixing ratio of cloud water, rainwater, cloud ice, graupel, and snow aggregates are plotted in fading white, yellow, blue, red, and green, respectively. The symbols indicate examples of unrealistic predicted ice particles (Sects. 7.3 and 9.1). See also Movie 1 in the video supplement.

- Eulerian component: momentum, heat, moisture budget
- Lagrangian component: super particles representing aerosol, water droplets, ice particles (porous spheroids)
- particle-resolved processes:
  — advection and sedimentation
  — homogeneous and immersion freezing (singular)
  — melting
  — condensation and evaporation (incl. CCN [de]activation)
  — deposition and sublimation
  — collisions (coalescence, riming, aggregation, washout)
- 2D Cb test case

Shima et al. ’20 particle-based mixed-phase μ-physics

Shima, Sato, Hashimoto & Misumi 2020 (GMD):

Predicting the morphology of ice particles in deep convection using the super-droplet method

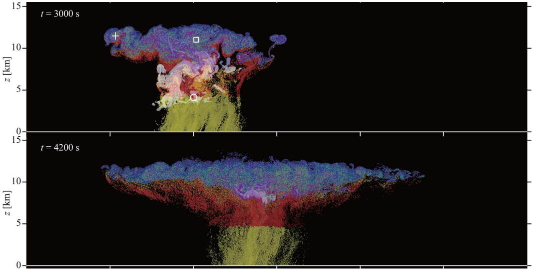

Figure 1. Typical realization of CTRL cloud spatial structures at $t = 2040$, 2460, 3000, 4200, and 5400 s. The mixing ratio of cloud water, rainwater, cloud ice, graupel, and snow aggregates are plotted in fading white, yellow, blue, red, and green, respectively. The symbols indicate examples of unrealistic predicted ice particles (Sects. 7.3 and 9.1). See also Movie 1 in the video supplement.

- Eulerian component: momentum, heat, moisture budget
- Lagrangian component: super particles representing aerosol, water droplets, ice particles (porous spheroids)
- particle-resolved processes:
  — advection and sedimentation
  — homogeneous and **immersion freezing (singular)**
  — melting
  — condensation and evaporation (incl. CCN [de]activation)
  — deposition and sublimation
  — collisions (coalescence, riming, aggregation, washout)
- 2D Cb test case

immersion freezing and other ice crystal formation pathways in clouds

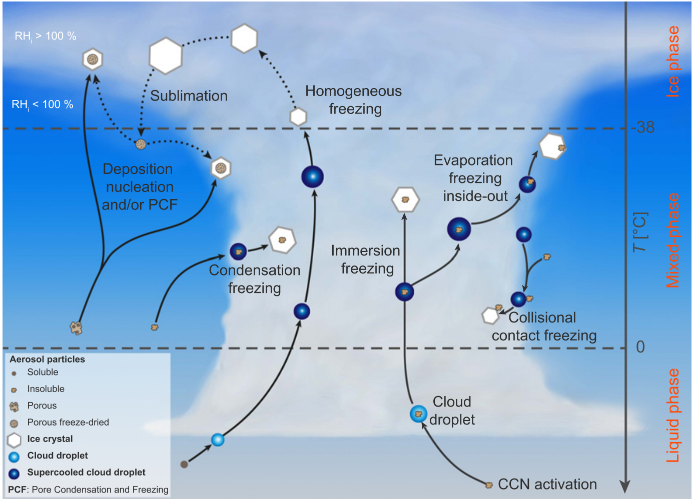

Kanji et al. 2017, graphics F. Mahrt, https://doi.org/10.1175/AMSMONOGRAPHS-D-16-0006.1

immersion freezing: bacteria and the Olympics

Journal of Geophysical Research: Atmospheres

RESEARCH ARTICLE

10.1002/2016JD025251

Key Points:

- Very ice active Snomax protein aggregates are fragile and their ice nucleation ability decreases over months of freezer storage
- Partitioning of ice active protein aggregates into the immersion oil reduces the droplet's measured freezing temperature

The unstable ice nucleation properties of Snomax® bacterial particles

Michael Polen[1], **Emily Lawlis**[1], **and Ryan C. Sullivan**[1]

[1]Center for Atmospheric Particle Studies, Carnegie Mellon University, Pittsburgh, Pennsylvania, USA

Abstract Snomax® is often used as a surrogate for biological ice nucleating particles (INPs) and has recently been proposed as an INP standard for evaluating ice nucleation methods. We have found the immersion freezing properties of Snomax particles to be substantially unstable, observing a loss of ice nucleation ability

immersion freezing: bacteria and the Olympics

Journal of Geophysical Research: Atmospheres

RESEARCH ARTICLE

10.1002/2016JD025251

Key Points:

- Very ice active Snomax protein aggregates are fragile and their ice nucleation ability decreases over months of freezer storage
- Partitioning of ice active protein aggregates into the immersion oil reduces the droplet's measured freezing temperature
- Caution is warranted in the use of

The unstable ice nucleation properties of Snomax® bacterial particles

Michael Polen[1], Emily Lawlis[1], and Ryan C. Sullivan[1]

[1]Center for Atmospheric Particle Studies, Carnegie Mellon University, Pittsburgh, Pennsylvania, USA

Abstract Snomax® is often used as a surrogate for biological ice nucleating particles (INPs) and has recently been proposed as an INP standard for evaluating ice nucleation methods. We have found the immersion freezing properties of Snomax particles to be substantially unstable, observing a loss of ice nucleation ability

https://www.reuters.com/markets/commodities/making-snow-stick-wind-challenges-winter-games-slope-makers-2021-11-29/

immersion freezing and other ice crystal formation pathways in clouds

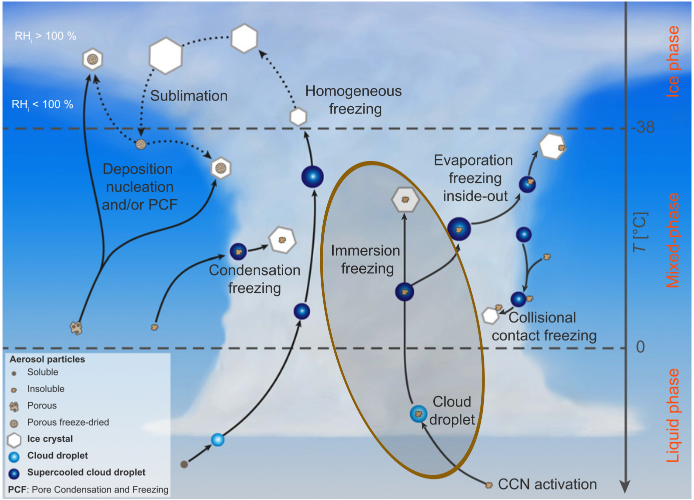

Kanji et al. 2017, graphics F. Mahrt, https://doi.org/10.1175/AMSMONOGRAPHS-D-16-0006.1

immersion freezing and other ice crystal formation pathways in clouds

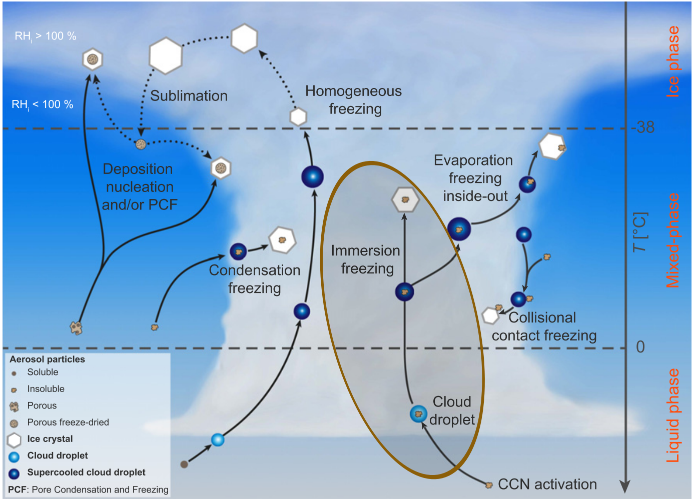

Kanji et al. 2017, graphics F. Mahrt, `https://doi.org/10.1175/AMSMONOGRAPHS-D-16-0006.1`

Vonnegut 1948 (J. Colloid Sci.)

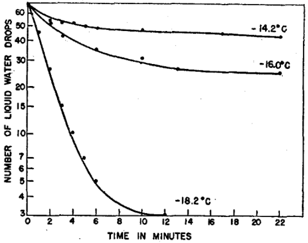

Fraction of water drops remaining unfrozen as a function of time.

immersion freezing and other ice crystal formation pathways in clouds

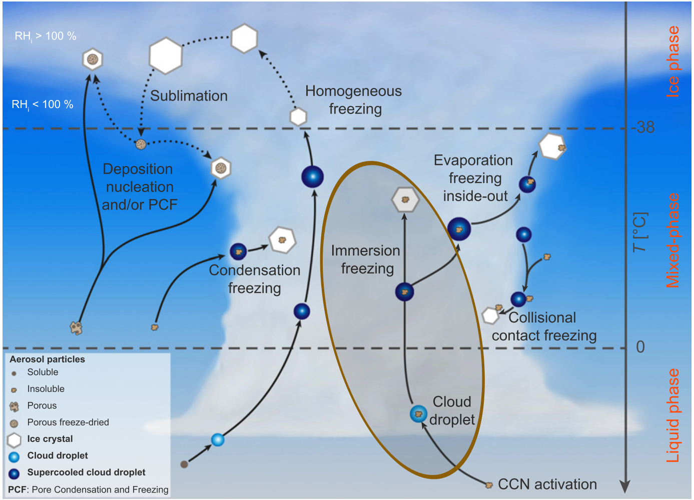

Kanji et al. 2017, graphics F. Mahrt, `https://doi.org/10.1175/AMSMONOGRAPHS-D-16-0006.1`

Vonnegut 1948 (J. Colloid Sci.)

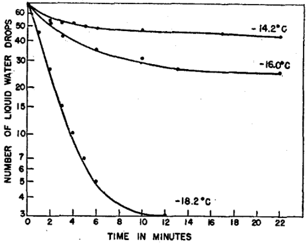

Fraction of water drops remaining unfrozen as a function of time.

Vali 2014 (ACP)

"Interpretations of the experimental results face considerable difficulties … two separate ways of interpreting the same observations; one assigned primacy to time the other emphasized the temperature-dependent impacts of the impurities … dichotomy – the stochastic and singular models"

Marshall et al. 1961 (Nubila 4(1))

Heterogeneous Nucleations is a Stochastic Process

by

J. S. MARSHALL

McGill University, Montreal, Canad.

Presented at the International Congress on the Physics of Clouds (Hailstorms) at Verona 9-13 August 1960.

http://cma.entecra.it/Astro2_sito/doc/Nubila_1_1961.pdf

Poissonian model of freezing & Ice Nucleation Active Sites (INAS)

theory (in modern notation)
(Bigg '53, Langham & Mason '58, Carte '59, Marshall '61)

Poissonian model of freezing & Ice Nucleation Active Sites (INAS)

theory (in modern notation)
(Bigg '53, Langham & Mason '58, Carte '59, Marshall '61)

Poisson counting process with rate r:

$$P^*(\text{k events in time t}) = \frac{(rt)^k \exp(-rt)}{k!}$$

$$P(\text{one or more events in time t}) = 1 - P^*(k = 0, t)$$

$$\ln(1 - P) = -rt$$

Poissonian model of freezing & Ice Nucleation Active Sites (INAS)

theory (in modern notation)
(Bigg '53, Langham & Mason '58, Carte '59, Marshall '61)

Poisson counting process with rate r:

$$P^*(\text{k events in time t}) = \frac{(rt)^k \exp(-rt)}{k!}$$

$$P(\text{one or more events in time t}) = 1 - P^*(k = 0, t)$$

$$\ln(1 - P) = -rt$$

introducing $J_{het}(T)$, $T(t)$ and INP surface A:

$$\ln(1 - P(A, t)) = -A \underbrace{\int_0^t J_{het}(T(t'))\, dt'}_{I(T)}$$

Poissonian model of freezing & Ice Nucleation Active Sites (INAS)

theory (in modern notation)
(Bigg '53, Langham & Mason '58, Carte '59, Marshall '61)

Poisson counting process with rate r:

$$P^*(\text{k events in time t}) = \frac{(rt)^k \exp(-rt)}{k!}$$

$$P(\text{one or more events in time t}) = 1 - P^*(k=0, t)$$

$$\ln(1-P) = -rt$$

introducing $J_{\text{het}}(T)$, $T(t)$ and INP surface A:

$$\ln\left(1 - P(A,t)\right) = -A \underbrace{\int_0^t J_{\text{het}}(T(t'))\,dt'}_{I(T)}$$

INAS: $$I(T) = n_s(T) = \exp(a \cdot (T - T_{0^\circ C}) + b)$$

Poissonian model of freezing & Ice Nucleation Active Sites (INAS)

theory (in modern notation)
(Bigg '53, Langham & Mason '58, Carte '59, Marshall '61)

Poisson counting process with rate r:

$$P^*(\text{k events in time t}) = \frac{(rt)^k \exp(-rt)}{k!}$$

$$P(\text{one or more events in time t}) = 1 - P^*(k=0, t)$$

$$\ln(1-P) = -rt$$

introducing $J_{\text{het}}(T)$, $T(t)$ and INP surface A:

$$\ln\left(1 - P(A,t)\right) = -A \underbrace{\int_0^t J_{\text{het}}(T(t'))\, dt'}_{I(T)}$$

INAS: $I(T) = n_s(T) = \exp(a \cdot (T - T_{0^\circ C}) + b)$

experimental $n_s(T)$ fits: e.g., Niemand et al. 2012

particle-based Monte-Carlo freezing: singular vs. time-dependent

singular[1]: INAS T_{fz} **as attribute**; initialisation by random sampling from $P(T_{fz}, A)$ with lognormal A (A is not an attribute, initialisation only); freezing if $T(t) < T_{fz}(t = 0)$

time-dependent[2]: A **as attribute** (randomly sampled from the same lognormal) Monte-Carlo freezing trigger using $P(J_{het}(T(t)))$

singular (INAS)

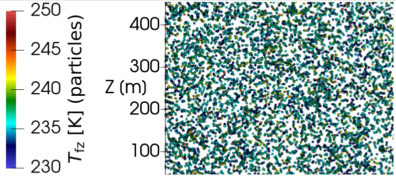

time-dependent (ABIFM)

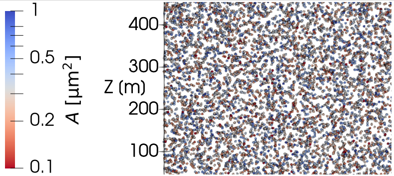

particle-based Monte-Carlo freezing: singular vs. time-dependent

singular[1]: INAS T_{fz} **as attribute**; initialisation by random sampling from $P(T_{\text{fz}}, A)$ with lognormal A (A is not an attribute, initialisation only); freezing if $T(t) < T_{fz}(t = 0)$

time-dependent[2]: A **as attribute** (randomly sampled from the same lognormal) Monte-Carlo freezing trigger using $P(J_{\text{het}}(T(t)))$

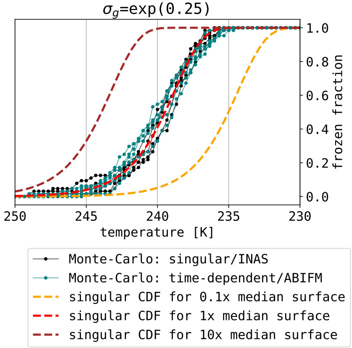

[1] as in Shima et al. 2020, GMD: doi: 10.5194/gmd-13-4107-2020
[2] as in Knopf & Alpert 2016, ACP: doi: 10.5194/acp-16-2083-2016

particle-based Monte-Carlo freezing: singular vs. time-dependent

singular[1]: INAS T_{fz} **as attribute**; initialisation by random sampling from $P(T_{fz}, A)$ with lognormal A (A is not an attribute, initialisation only); freezing if $T(t) < T_{fz}(t = 0)$

time-dependent[2]: A **as attribute** (randomly sampled from the same lognormal) Monte-Carlo freezing trigger using $P(J_{het}(T(t)))$

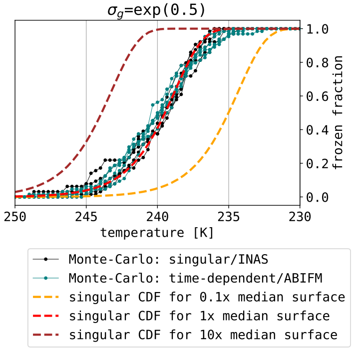

[1] as in Shima et al. 2020, GMD: doi: 10.5194/gmd-13-4107-2020
[2] as in Knopf & Alpert 2016, ACP: doi: 10.5194/acp-16-2083-2016

particle-based Monte-Carlo freezing: singular vs. time-dependent

singular[1]: INAS T_{fz} **as attribute**; initialisation by random sampling from $P(T_{fz}, A)$ with lognormal A (A is not an attribute, initialisation only); freezing if $T(t) < T_{fz}(t=0)$

time-dependent[2]: A **as attribute** (randomly sampled from the same lognormal) Monte-Carlo freezing trigger using $P(J_{het}(T(t)))$

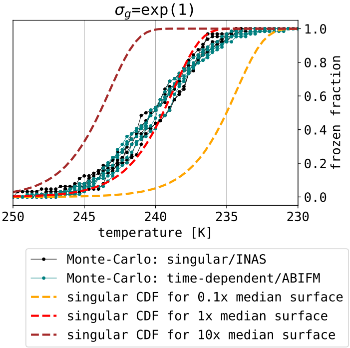

[1] as in Shima et al. 2020, GMD: doi: 10.5194/gmd-13-4107-2020
[2] as in Knopf & Alpert 2016, ACP: doi: 10.5194/acp-16-2083-2016

particle-based Monte-Carlo freezing: singular vs. time-dependent

singular[1]: INAS T_{fz} **as attribute**; initialisation by random sampling from $P(T_{fz}, A)$ with lognormal A (A is not an attribute, initialisation only); freezing if $T(t) < T_{fz}(t=0)$

time-dependent[2]: A **as attribute** (randomly sampled from the same lognormal) Monte-Carlo freezing trigger using $P(J_{het}(T(t)))$

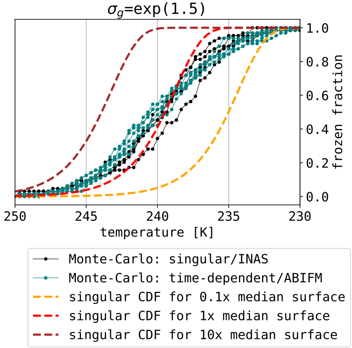

[1] as in Shima et al. 2020, GMD: doi: 10.5194/gmd-13-4107-2020
[2] as in Knopf & Alpert 2016, ACP: doi: 10.5194/acp-16-2083-2016

particle-based Monte-Carlo freezing: singular vs. time-dependent

singular[1]: INAS T_{fz} **as attribute**; initialisation by random sampling from $P(T_{\mathrm{fz}}, A)$ with lognormal A (A is not an attribute, initialisation only); freezing if $T(t) < T_{fz}(t=0)$

time-dependent[2]: A **as attribute** (randomly sampled from the same lognormal) Monte-Carlo freezing trigger using $P(J_{\mathrm{het}}(T(t)))$

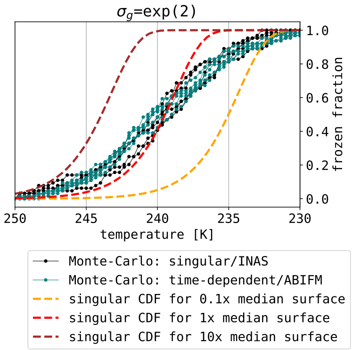

[1] as in Shima et al. 2020, GMD: doi: 10.5194/gmd-13-4107-2020
[2] as in Knopf & Alpert 2016, ACP: doi: 10.5194/acp-16-2083-2016

particle-based Monte-Carlo freezing: singular vs. time-dependent

singular[1]: INAS T_{fz} **as attribute**; initialisation by random sampling from $P(T_{fz}, A)$ with lognormal A (A is not an attribute, initialisation only); freezing if $T(t) < T_{fz}(t=0)$

time-dependent[2]: A **as attribute** (randomly sampled from the same lognormal) Monte-Carlo freezing trigger using $P(J_{het}(T(t)))$

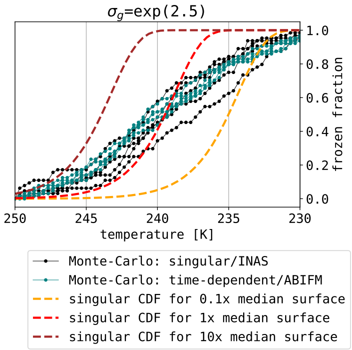

[1] as in Shima et al. 2020, GMD: doi: 10.5194/gmd-13-4107-2020
[2] as in Knopf & Alpert 2016, ACP: doi: 10.5194/acp-16-2083-2016

particle-based Monte-Carlo freezing: singular vs. time-dependent

singular[1]: INAS T_{fz} **as attribute**; initialisation by random sampling from $P(T_{fz}, A)$ with lognormal A (A is not an attribute, initialisation only); freezing if $T(t) < T_{fz}(t=0)$

time-dependent[2]: A **as attribute** (randomly sampled from the same lognormal) Monte-Carlo freezing trigger using $P(J_{het}(T(t)))$

AIDA cooling rate: $0.5\,{}^{K}/_{min}$

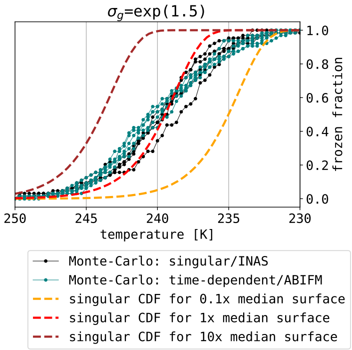

[1] as in Shima et al. 2020, GMD: doi: 10.5194/gmd-13-4107-2020
[2] as in Knopf & Alpert 2016, ACP: doi: 10.5194/acp-16-2083-2016

particle-based Monte-Carlo freezing: singular vs. time-dependent

singular[1]: INAS T_{fz} **as attribute**; initialisation by random sampling from $P(T_{fz}, A)$ with lognormal A (A is not an attribute, initialisation only); freezing if $T(t) < T_{fz}(t=0)$

time-dependent[2]: A **as attribute** (randomly sampled from the same lognormal) Monte-Carlo freezing trigger using $P(J_{het}(T(t)))$

cooling rate: $0.1\ ^{K}/_{min}$

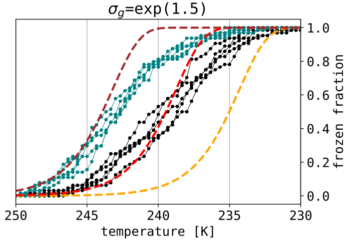

AIDA cooling rate: $0.5\ ^{K}/_{min}$

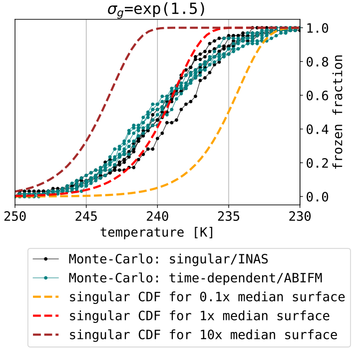

[1] as in Shima et al. 2020, GMD: doi: 10.5194/gmd-13-4107-2020
[2] as in Knopf & Alpert 2016, ACP: doi: 10.5194/acp-16-2083-2016

particle-based Monte-Carlo freezing: singular vs. time-dependent

singular[1]: INAS T_{fz} **as attribute**; initialisation by random sampling from $P(T_{\rm fz}, A)$ with lognormal A (A is not an attribute, initialisation only); freezing if $T(t) < T_{fz}(t=0)$

time-dependent[2]: A **as attribute** (randomly sampled from the same lognormal) Monte-Carlo freezing trigger using $P(J_{\rm het}(T(t)))$

cooling rate: 0.1 $^K/_{min}$	AIDA cooling rate: 0.5 $^K/_{min}$	cooling rate: 2.5 $^K/_{min}$

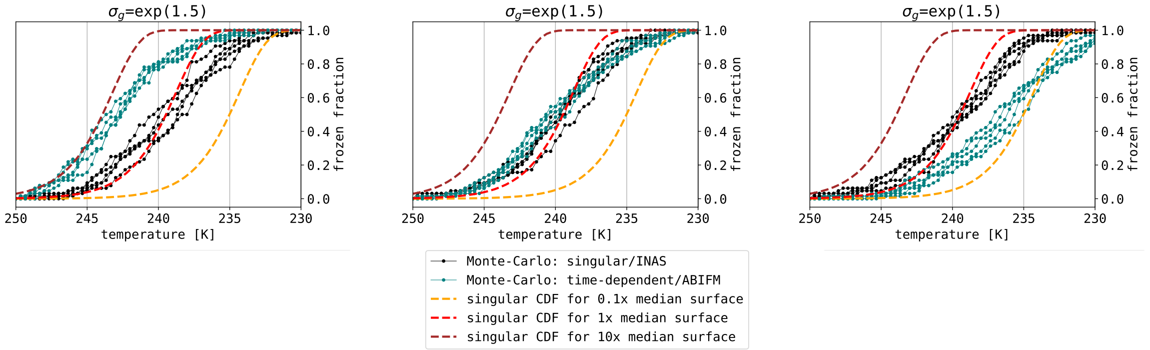

[1] as in Shima et al. 2020, GMD: doi: 10.5194/gmd-13-4107-2020

[2] as in Knopf & Alpert 2016, ACP: doi: 10.5194/acp-16-2083-2016

Poissonian model of freezing & Ice Nucleation Active Sites (INAS)

theory (in modern notation)
(Bigg '53, Langham & Mason '58, Carte '59, Marshall '61)

Poisson counting process with rate r:

$$P^*(\text{k events in time t}) = \frac{(rt)^k \exp(-rt)}{k!}$$

$$P(\text{one or more events in time t}) = 1 - P^*(k=0, t)$$

$$\ln(1-P) = -rt$$

introducing $J_{het}(T)$, $T(t)$ and INP surface A:

$$\ln(1 - P(A,t)) = \underbrace{-A\int_0^t J_{het}(T(t'))\,dt'}_{I(T)}$$

INAS: $I(T) = n_s(T) = \exp(a \cdot (T - T_{0^\circ C}) + b)$

experimental $n_s(T)$ fits: e.g., Niemand et al. 2012

Poissonian model of freezing & Ice Nucleation Active Sites (INAS)

theory (in modern notation)
(Bigg '53, Langham & Mason '58, Carte '59, Marshall '61)

Poisson counting process with rate r:

$$P^*(\text{k events in time t}) = \frac{(rt)^k \exp(-rt)}{k!}$$

$$P(\text{one or more events in time t}) = 1 - P^*(k=0, t)$$

$$\ln(1-P) = -rt$$

introducing $J_{\text{het}}(T)$, $T(t)$ and INP surface A:

$$\ln\left(1-P(A,t)\right) = -A\underbrace{\int_0^t J_{\text{het}}(T(t'))\,dt'}_{I(T)}$$

INAS: $I(T) = n_s(T) = \exp(a \cdot (T - T_{0^\circ C}) + b)$

experimental $n_s(T)$ fits: e.g., Niemand et al. 2012

for a constant cooling rate $c = dT/dt$:

$$\ln(1-P(A,t)) = -\frac{A}{c}\int_{T_0}^{T_0+ct} J_{\text{het}}(T')dT' = -A \cdot I(T)$$

Poissonian model of freezing & Ice Nucleation Active Sites (INAS)

theory (in modern notation)
(Bigg '53, Langham & Mason '58, Carte '59, Marshall '61)

Poisson counting process with rate r:

$$P^*(\text{k events in time t}) = \frac{(rt)^k \exp(-rt)}{k!}$$

$$P(\text{one or more events in time t}) = 1 - P^*(k=0, t)$$

$$\ln(1-P) = -rt$$

introducing $J_{het}(T)$, $T(t)$ and INP surface A:

$$\ln\left(1-P(A,t)\right) = -A \underbrace{\int_0^t J_{het}(T(t'))\, dt'}_{I(T)}$$

INAS: $I(T) = n_s(T) = \exp(a \cdot (T - T_{0°C}) + b)$

experimental $n_s(T)$ fits: e.g., Niemand et al. 2012

for a constant cooling rate $c = dT/dt$:

$$\ln(1 - P(A,t)) = -\frac{A}{c}\int_{T_0}^{T_0+ct} J_{het}(T')dT' = -A \cdot I(T)$$

$$\frac{dn_s(T)}{dT} = a \cdot n_s(T) = -\frac{1}{c} J_{het}(T)$$

Poissonian model of freezing & Ice Nucleation Active Sites (INAS)

theory (in modern notation)
(Bigg '53, Langham & Mason '58, Carte '59, Marshall '61)

Poisson counting process with rate r:

$$P^*(\text{k events in time t}) = \frac{(rt)^k \exp(-rt)}{k!}$$

$$P(\text{one or more events in time t}) = 1 - P^*(k=0, t)$$

$$\ln(1-P) = -rt$$

introducing $J_{het}(T)$, $T(t)$ and INP surface A:

$$\ln\left(1-P(A,t)\right) = -A\underbrace{\int_0^t J_{het}(T(t'))\,dt'}_{I(T)}$$

INAS: $I(T) = n_s(T) = \exp(a \cdot (T - T_{0°C}) + b)$

experimental $n_s(T)$ fits: e.g., Niemand et al. 2012

for a constant cooling rate $c = dT/dt$:

$$\ln(1-P(A,t)) = -\frac{A}{c}\int_{T_0}^{T_0+ct} J_{het}(T')dT' = -A \cdot I(T)$$

$$\frac{dn_s(T)}{dT} = a \cdot n_s(T) = -\frac{1}{c}J_{het}(T)$$

experimental fits: INAS n_s (Niemand et al. '12)
ABIFM J_{het} (Knopf & Alpert '13)

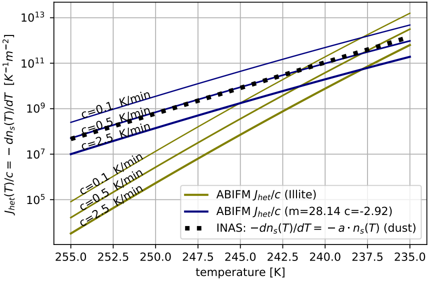

Poissonian model of freezing & Ice Nucleation Active Sites (INAS)

theory (in modern notation)
(Bigg '53, Langham & Mason '58, Carte '59, Marshall '61)

Poisson counting process with rate r:

$$P^*(\text{k events in time t}) = \frac{(rt)^k \exp(-rt)}{k!}$$

$$P(\text{one or more events in time t}) = 1 - P^*(k=0, t)$$

$$\ln(1-P) = -rt$$

introducing $J_{het}(T)$, $T(t)$ and INP surface A:

$$\ln\left(1-P(A,t)\right) = \underbrace{-A\int_0^t J_{het}(T(t'))\,dt'}_{I(T)}$$

INAS: $\quad I(T) = n_s(T) = \exp(a \cdot (T - T_{0°C}) + b)$

experimental $n_s(T)$ fits: e.g., Niemand et al. 2012

for a constant cooling rate $c = dT/dt$:

$$\ln(1-P(A,t)) = -\frac{A}{c}\int_{T_0}^{T_0+ct} J_{het}(T')dT' = -A \cdot I(T)$$

$$\frac{dn_s(T)}{dT} = a \cdot n_s(T) = -\frac{1}{c}J_{het}(T)$$

experimental fits: INAS n_s (Niemand et al. '12)
ABIFM J_{het} (Knopf & Alpert '13)

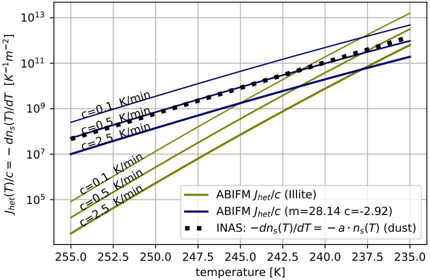

cf. Vali & Stansbury '66; modified singular model (Vali '94, Murray et al. '11)
but the singular ansatz limitation of sampling T_{fz} at t=0 remains

Poissonian model of freezing & Ice Nucleation Active Sites (INAS)

Is it a problem?

for a constant cooling rate $c = dT/dt$:

$$\ln(1 - P(A,t)) = -\frac{A}{c}\int_{T_0}^{T_0+ct} J_{\text{het}}(T')dT' = -A \cdot I(T)$$

$$\frac{dn_s(T)}{dT} = a \cdot n_s(T) = -\frac{1}{c} J_{\text{het}}(T)$$

experimental fits: INAS n_s (Niemand et al. '12)
ABIFM J_{het} (Knopf & Alpert '13)

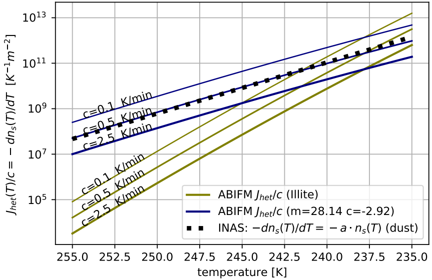

cf. Vali & Stansbury '66; modified singular model (Vali '94, Murray et al. '11)
but the singular ansatz limitation of sampling T_{fz} at t=0 remains

particle-based μ-physics + prescribed-flow test (aka KiD-2D)[a,b,c,d,e,f]

Lagrangian component (PySDM)

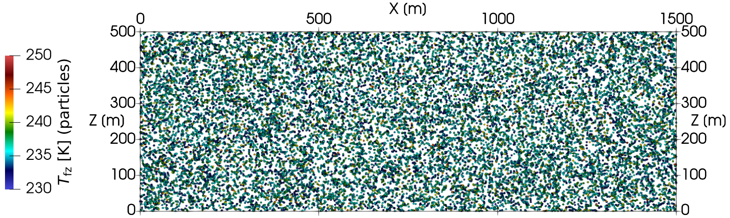

Eulerian component (PyMPDATA)

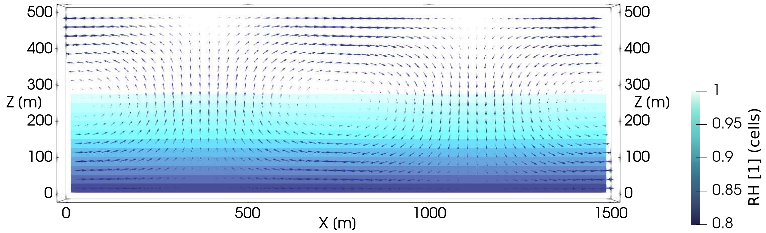

[a] concept: Gedzelman & Arnold '93

[b] stratiform: Morrison & Grabowski '07

[c] ice phase: e.g., Yang et al. '15

[d] particle-based: e.g., Arabas et al. '15

[e] KiD-2D: github.com/BShipway/KiD

[f] here: SHEBA case (Fridlind et al. '12)

particle-based μ-physics + prescribed-flow test

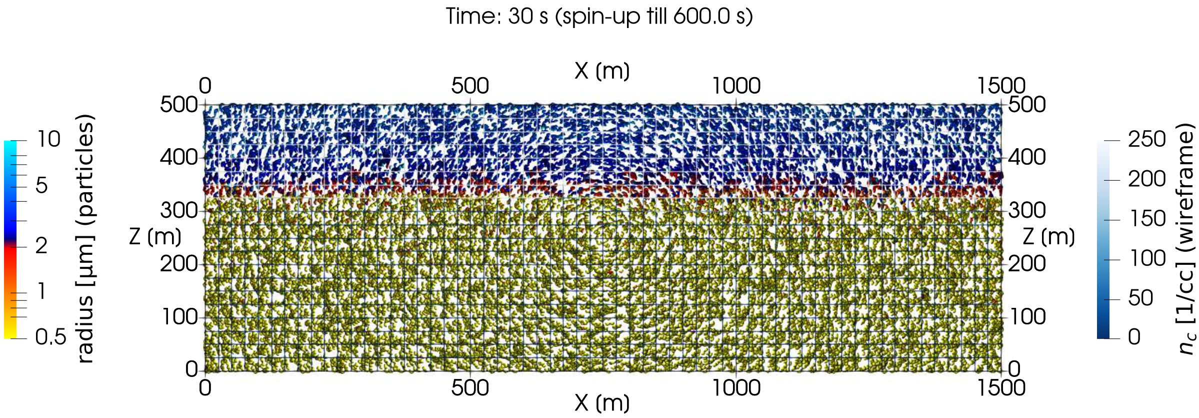

16+16 super-particles/cell for INP-rich + INP-free particles

$N_{aer} = 300/cc$ (two-mode lognormal) $N_{INP} = 150/L$ (lognormal, $D_g = 0.74$ μm, $\sigma_g = 2.55$)

spin-up = freezing off; subsequently frozen particles act as tracers

particle-based μ-physics + prescribed-flow test

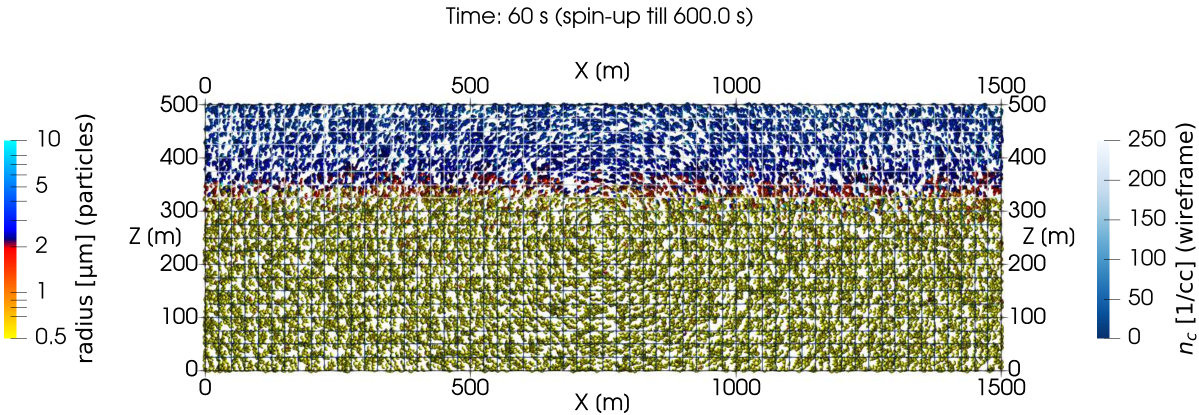

16+16 super-particles/cell for INP-rich + INP-free particles

$N_{aer} = 300/cc$ (two-mode lognormal) $N_{INP} = 150/L$ (lognormal, $D_g = 0.74$ μm, $\sigma_g = 2.55$)

spin-up = freezing off; subsequently frozen particles act as tracers

particle-based μ-physics + prescribed-flow test

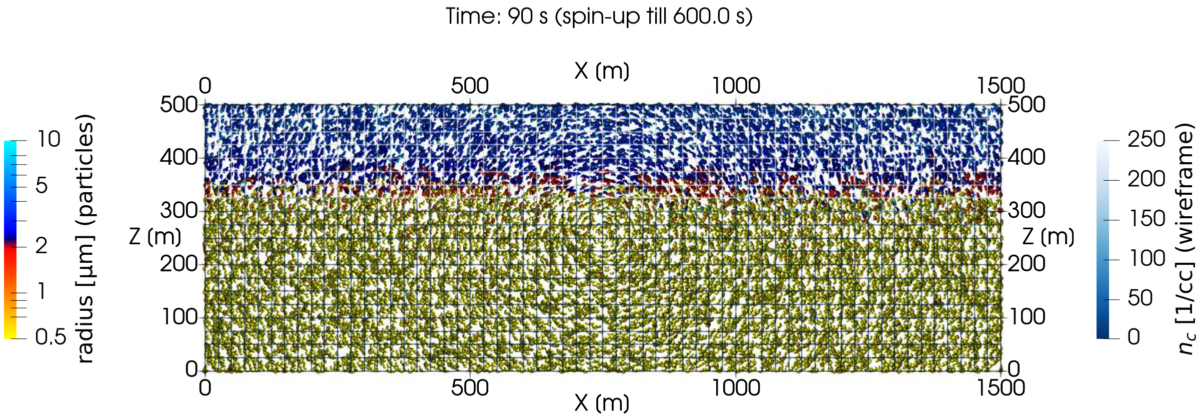

16+16 super-particles/cell for INP-rich + INP-free particles

$N_{\text{aer}} = 300/cc$ (two-mode lognormal) $N_{\text{INP}} = 150/L$ (lognormal, $D_g = 0.74$ μm, $\sigma_g = 2.55$)

spin-up = freezing off; subsequently frozen particles act as tracers

particle-based μ-physics + prescribed-flow test

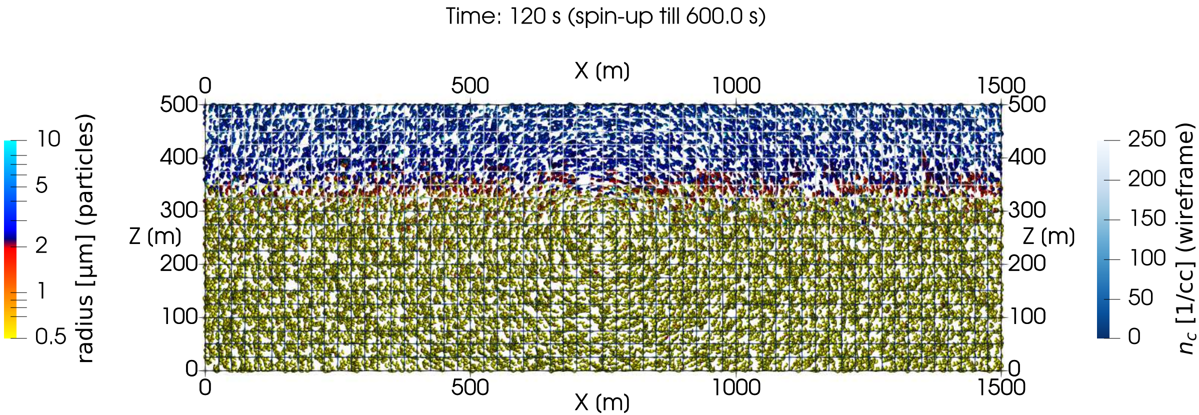

16+16 super-particles/cell for INP-rich + INP-free particles

$N_{aer} = 300/cc$ (two-mode lognormal) $N_{INP} = 150/L$ (lognormal, $D_g = 0.74$ μm, $\sigma_g = 2.55$)

spin-up = freezing off; subsequently frozen particles act as tracers

particle-based µ-physics + prescribed-flow test

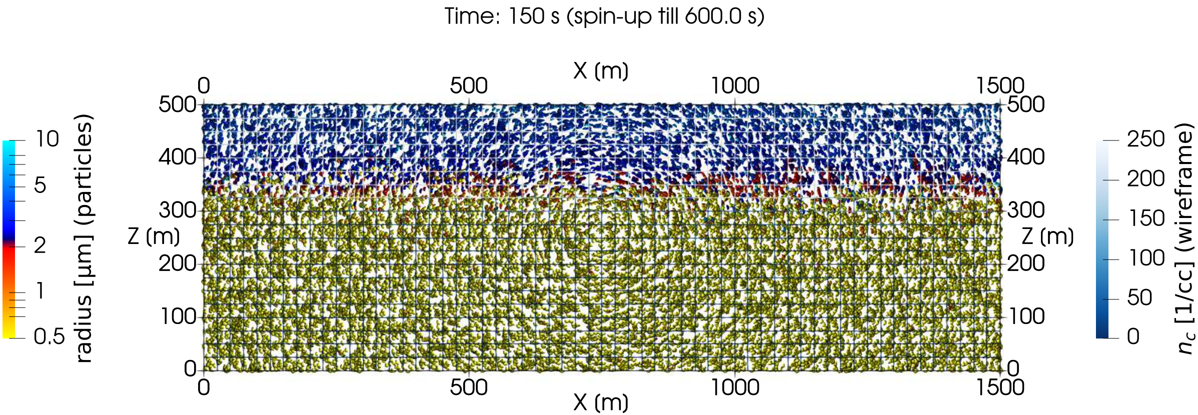

16+16 super-particles/cell for INP-rich + INP-free particles

$N_{aer} = 300/cc$ (two-mode lognormal) $N_{INP} = 150/L$ (lognormal, $D_g = 0.74$ µm, $\sigma_g = 2.55$)

spin-up = freezing off; subsequently frozen particles act as tracers

particle-based μ-physics + prescribed-flow test

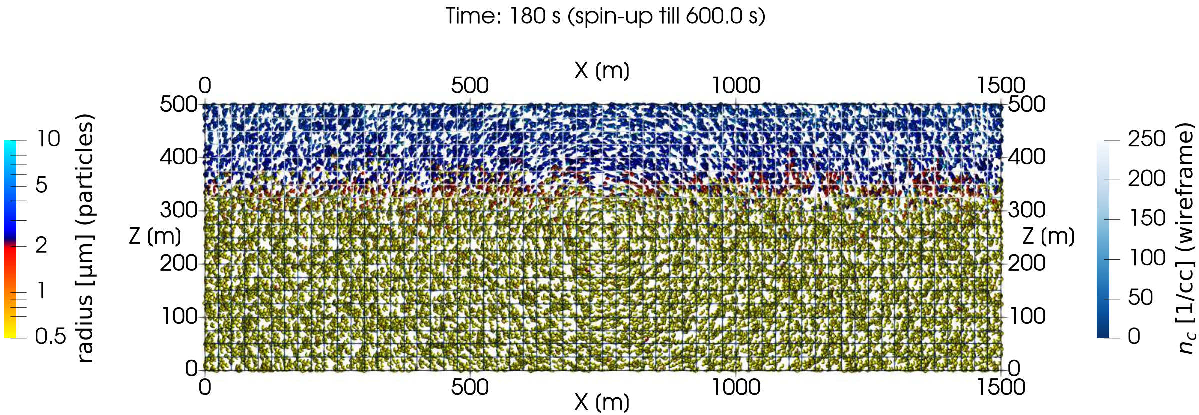

16+16 super-particles/cell for INP-rich + INP-free particles

$N_{\text{aer}} = 300/cc$ (two-mode lognormal) $N_{\text{INP}} = 150/L$ (lognormal, $D_g = 0.74$ μm, $\sigma_g = 2.55$)

spin-up = freezing off; subsequently frozen particles act as tracers

particle-based μ-physics + prescribed-flow test

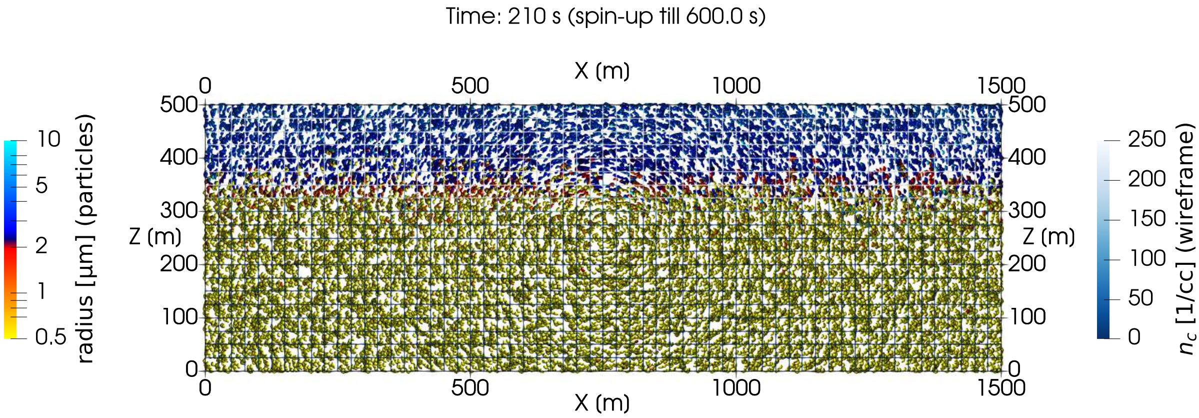

16+16 super-particles/cell for INP-rich + INP-free particles

N_{aer} = 300/*cc* (two-mode lognormal) N_{INP} = 150/*L* (lognormal, D_g =0.74 μm, σ_g =2.55)

spin-up = freezing off; subsequently frozen particles act as tracers

particle-based μ-physics + prescribed-flow test

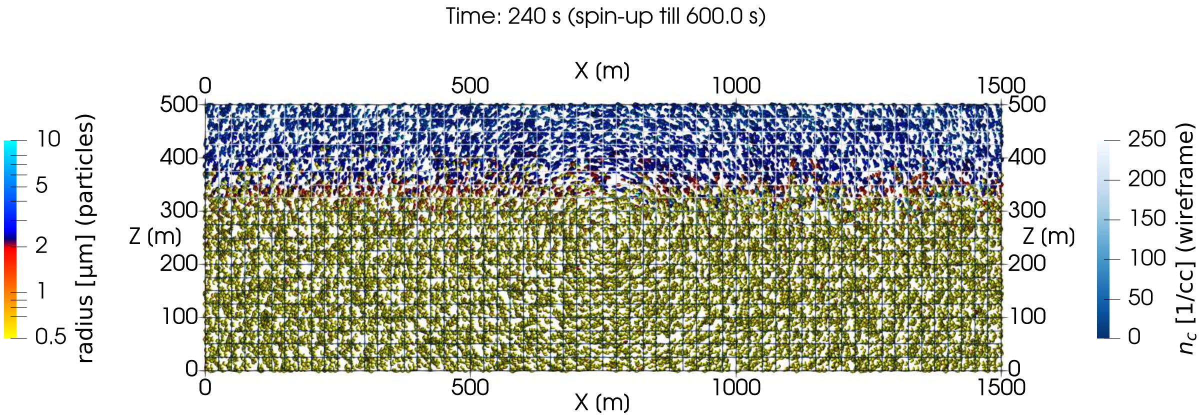

16+16 super-particles/cell for INP-rich + INP-free particles

$N_{\text{aer}} = 300/cc$ (two-mode lognormal) $N_{\text{INP}} = 150/L$ (lognormal, $D_g = 0.74$ μm, $\sigma_g = 2.55$)

spin-up = freezing off; subsequently frozen particles act as tracers

particle-based μ-physics + prescribed-flow test

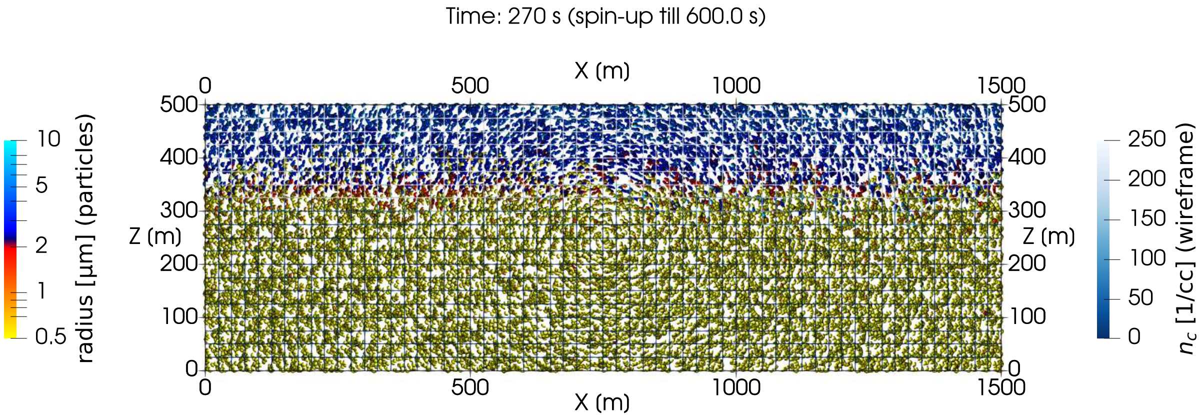

16+16 super-particles/cell for INP-rich + INP-free particles

$N_{\text{aer}} = 300/cc$ (two-mode lognormal) $N_{\text{INP}} = 150/L$ (lognormal, $D_g = 0.74$ μm, $\sigma_g = 2.55$)

spin-up = freezing off; subsequently frozen particles act as tracers

particle-based μ-physics + prescribed-flow test

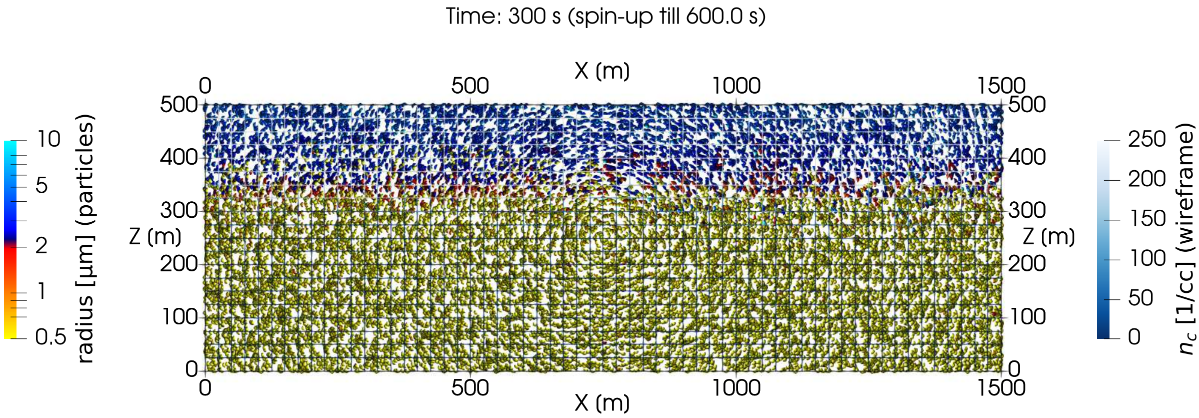

16+16 super-particles/cell for INP-rich + INP-free particles

$N_{aer} = 300/cc$ (two-mode lognormal) $N_{INP} = 150/L$ (lognormal, $D_g = 0.74$ μm, $\sigma_g = 2.55$)

spin-up = freezing off; subsequently frozen particles act as tracers

particle-based μ-physics + prescribed-flow test

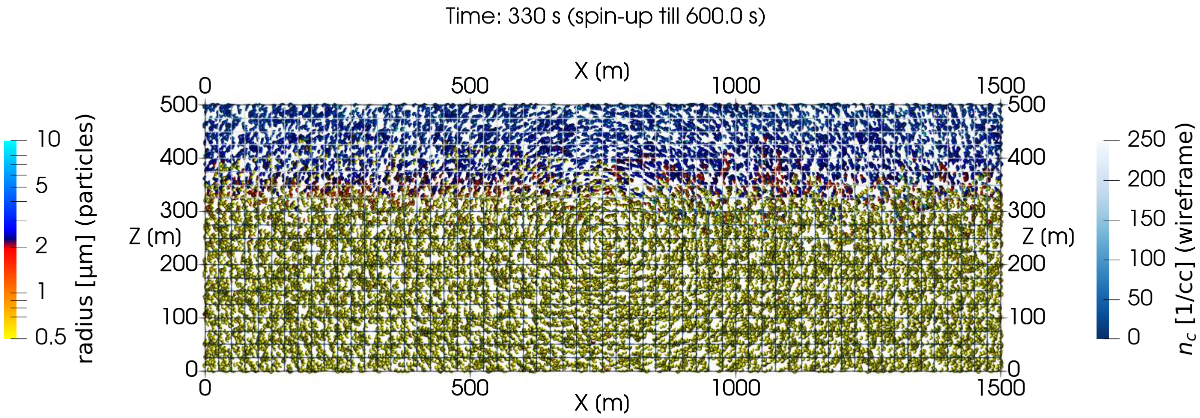

16+16 super-particles/cell for INP-rich + INP-free particles

$N_{aer} = 300/cc$ (two-mode lognormal) $N_{INP} = 150/L$ (lognormal, $D_g = 0.74$ μm, $\sigma_g = 2.55$)

spin-up = freezing off; subsequently frozen particles act as tracers

particle-based μ-physics + prescribed-flow test

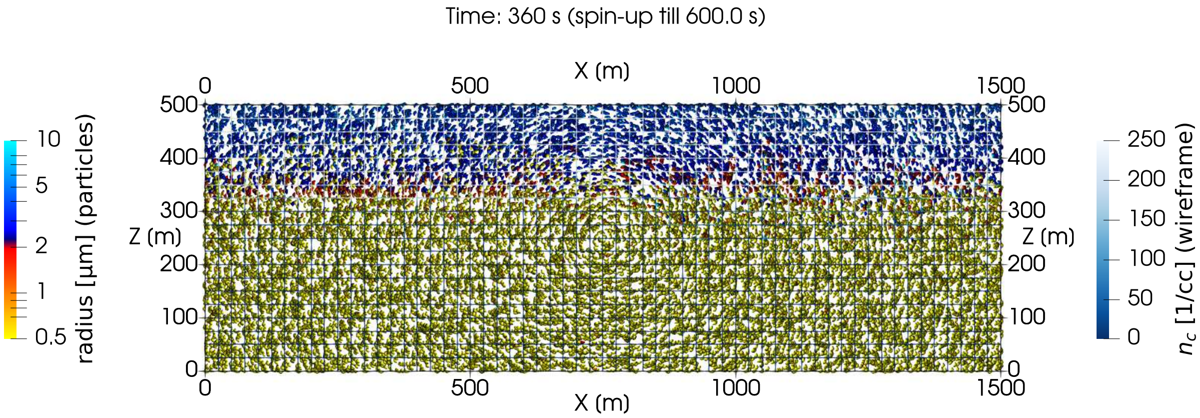

16+16 super-particles/cell for INP-rich + INP-free particles

$N_{aer} = 300/cc$ (two-mode lognormal) $N_{INP} = 150/L$ (lognormal, $D_g = 0.74$ μm, $\sigma_g = 2.55$)

spin-up = freezing off; subsequently frozen particles act as tracers

particle-based μ-physics + prescribed-flow test

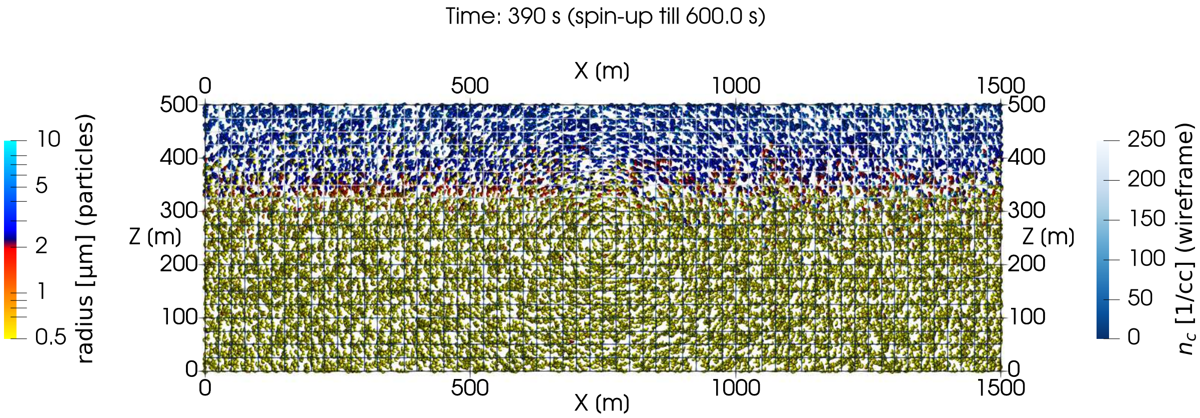

16+16 super-particles/cell for INP-rich + INP-free particles

$N_{aer} = 300/cc$ (two-mode lognormal) $N_{INP} = 150/L$ (lognormal, $D_g = 0.74$ μm, $\sigma_g = 2.55$)

spin-up = freezing off; subsequently frozen particles act as tracers

particle-based μ-physics + prescribed-flow test

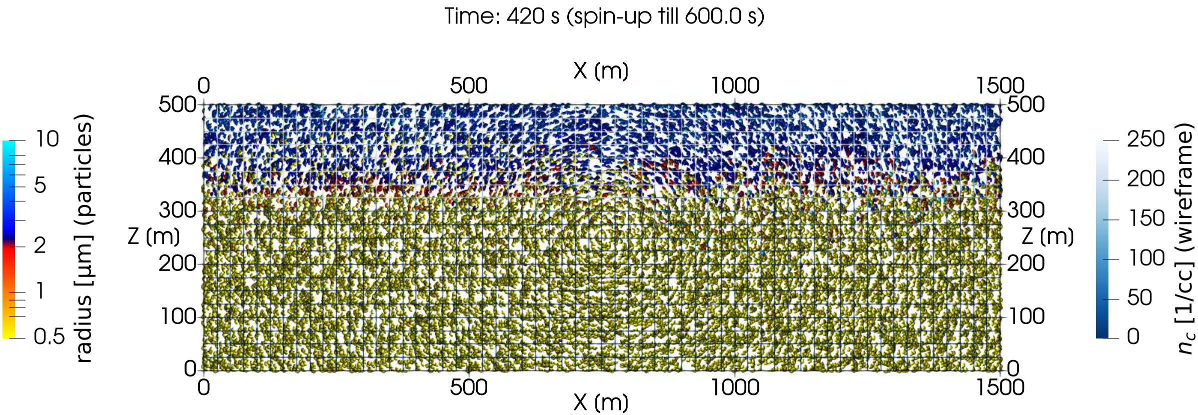

16+16 super-particles/cell for INP-rich + INP-free particles

$N_{\mathrm{aer}} = 300/cc$ (two-mode lognormal) $N_{\mathrm{INP}} = 150/L$ (lognormal, $D_g = 0.74$ μm, $\sigma_{\mathrm{g}} = 2.55$)

spin-up = freezing off; subsequently frozen particles act as tracers

particle-based μ-physics + prescribed-flow test

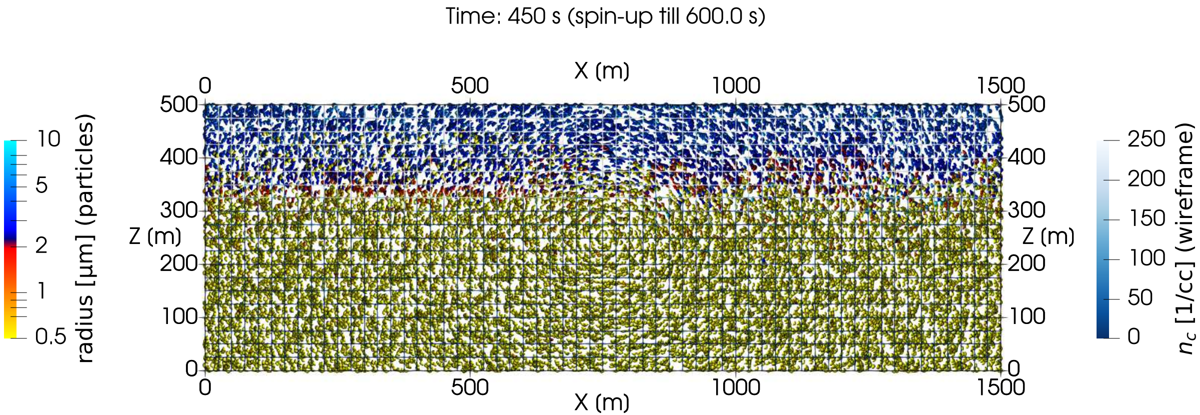

16+16 super-particles/cell for INP-rich + INP-free particles

$N_{aer} = 300/cc$ (two-mode lognormal) $N_{INP} = 150/L$ (lognormal, $D_g = 0.74$ μm, $\sigma_g = 2.55$)

spin-up = freezing off; subsequently frozen particles act as tracers

particle-based μ-physics + prescribed-flow test

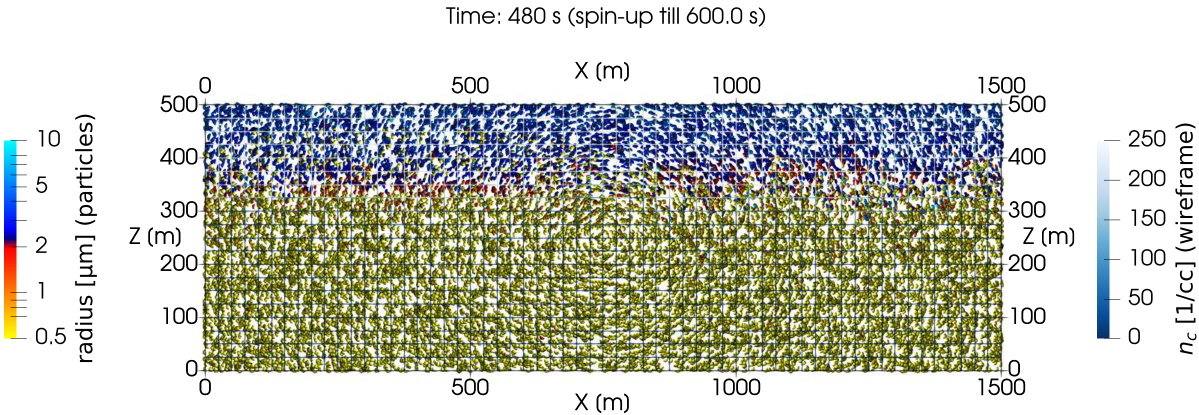

16+16 super-particles/cell for INP-rich + INP-free particles

$N_{aer} = 300/cc$ (two-mode lognormal) $N_{INP} = 150/L$ (lognormal, $D_g = 0.74$ μm, $\sigma_g = 2.55$)

spin-up = freezing off; subsequently frozen particles act as tracers

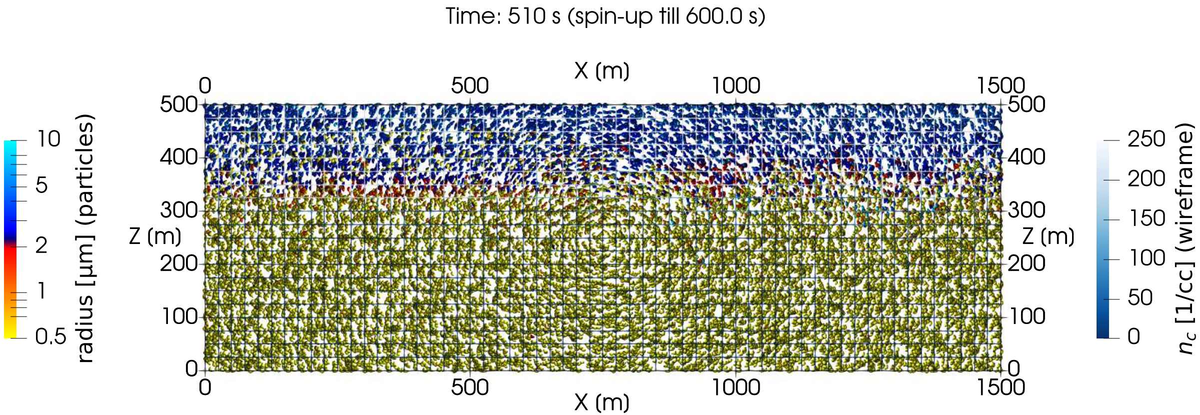

16+16 super-particles/cell for INP-rich + INP-free particles
$N_{\rm aer} = 300/cc$ (two-mode lognormal) $N_{\rm INP} = 150/L$ (lognormal, $D_g = 0.74$ μm, $\sigma_g = 2.55$)
spin-up = freezing off; subsequently frozen particles act as tracers

particle-based μ-physics + prescribed-flow test

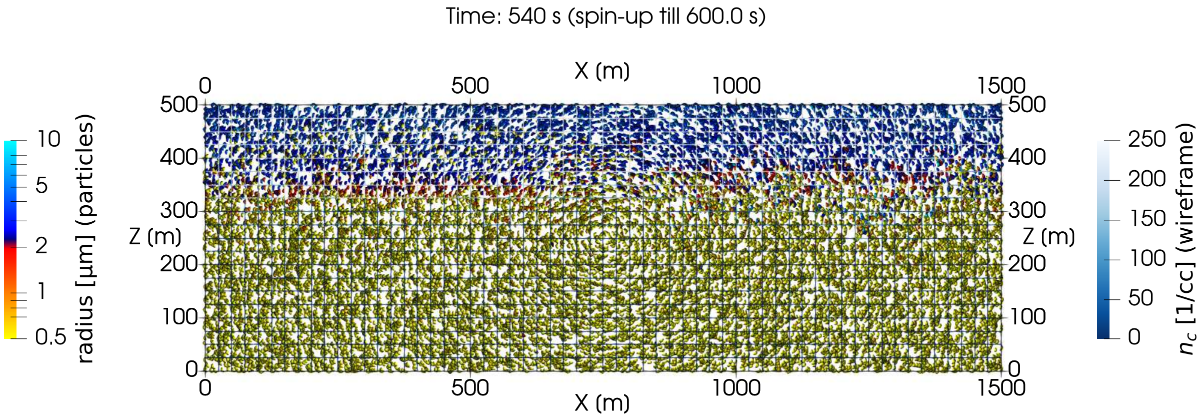

16+16 super-particles/cell for INP-rich + INP-free particles

$N_{\text{aer}} = 300/cc$ (two-mode lognormal) $N_{\text{INP}} = 150/L$ (lognormal, $D_g = 0.74$ μm, $\sigma_g = 2.55$)

spin-up = freezing off; subsequently frozen particles act as tracers

particle-based μ-physics + prescribed-flow test

Time: 570 s (spin-up till 600.0 s)

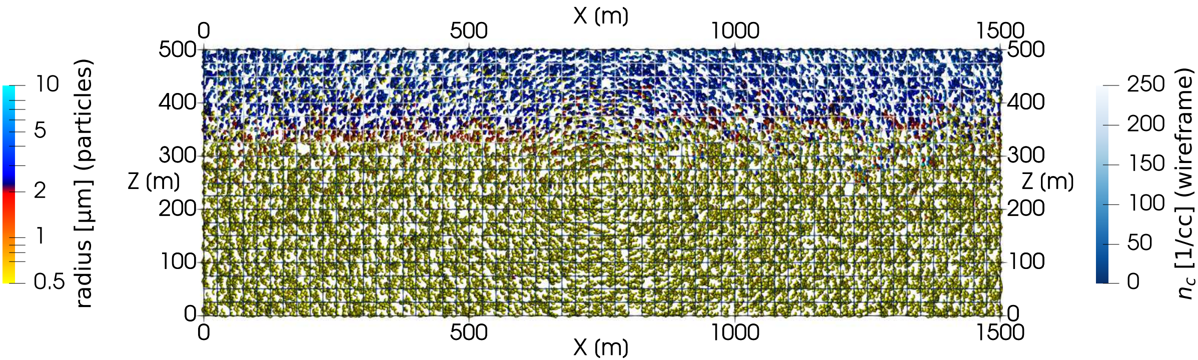

16+16 super-particles/cell for INP-rich + INP-free particles

$N_{aer} = 300/cc$ (two-mode lognormal) $N_{INP} = 150/L$ (lognormal, $D_g = 0.74$ μm, $\sigma_g = 2.55$)

spin-up = freezing off; subsequently frozen particles act as tracers

particle-based μ-physics + prescribed-flow test

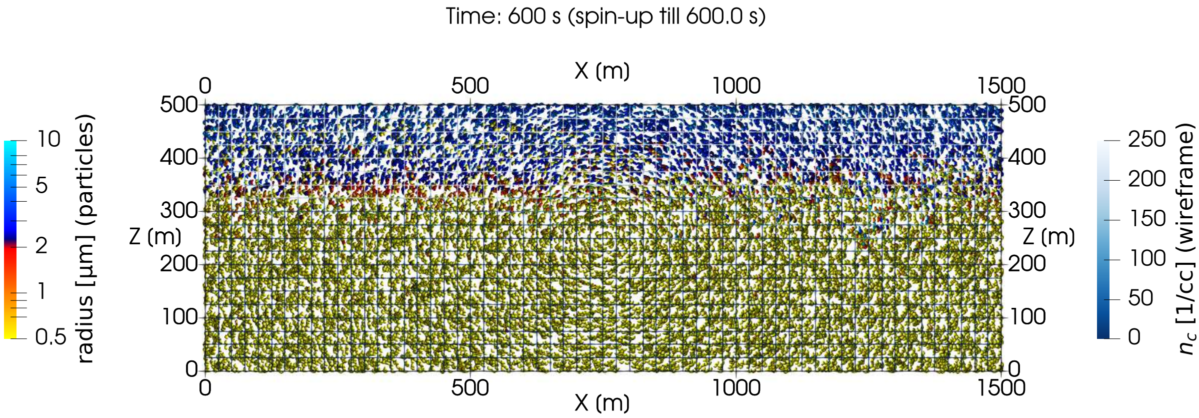

16+16 super-particles/cell for INP-rich + INP-free particles

$N_{aer} = 300/cc$ (two-mode lognormal) $N_{INP} = 150/L$ (lognormal, $D_g = 0.74$ μm, $\sigma_g = 2.55$)

spin-up = freezing off; subsequently frozen particles act as tracers

particle-based μ-physics + prescribed-flow test

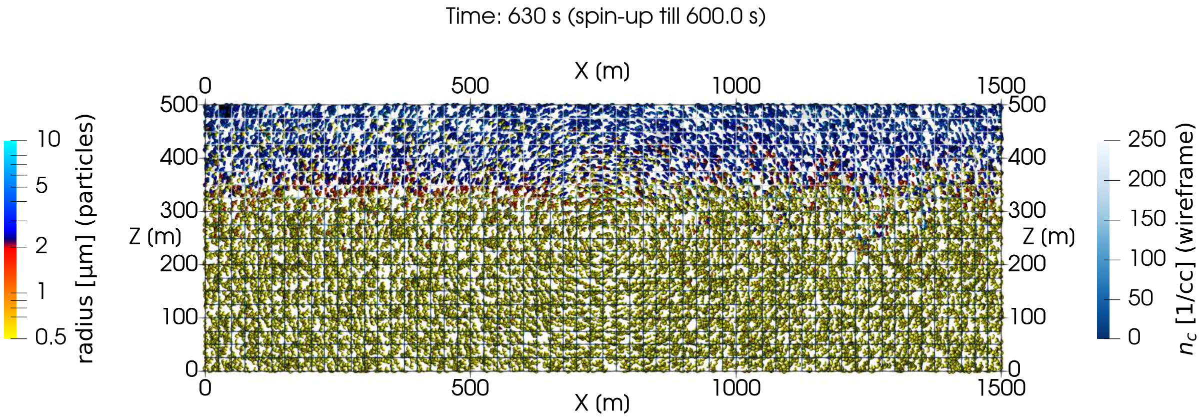

16+16 super-particles/cell for INP-rich + INP-free particles

$N_{aer} = 300/cc$ (two-mode lognormal) $N_{INP} = 150/L$ (lognormal, $D_g = 0.74$ μm, $\sigma_g = 2.55$)

spin-up = freezing off; subsequently frozen particles act as tracers

particle-based μ-physics + prescribed-flow test

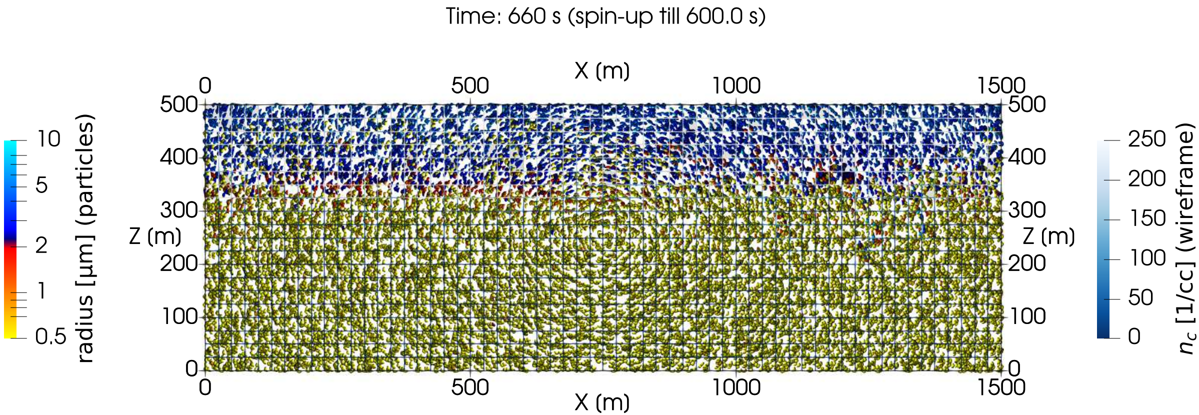

16+16 super-particles/cell for INP-rich + INP-free particles

$N_{aer} = 300/cc$ (two-mode lognormal) $N_{INP} = 150/L$ (lognormal, $D_g = 0.74$ μm, $\sigma_g = 2.55$)

spin-up = freezing off; subsequently frozen particles act as tracers

particle-based μ-physics + prescribed-flow test

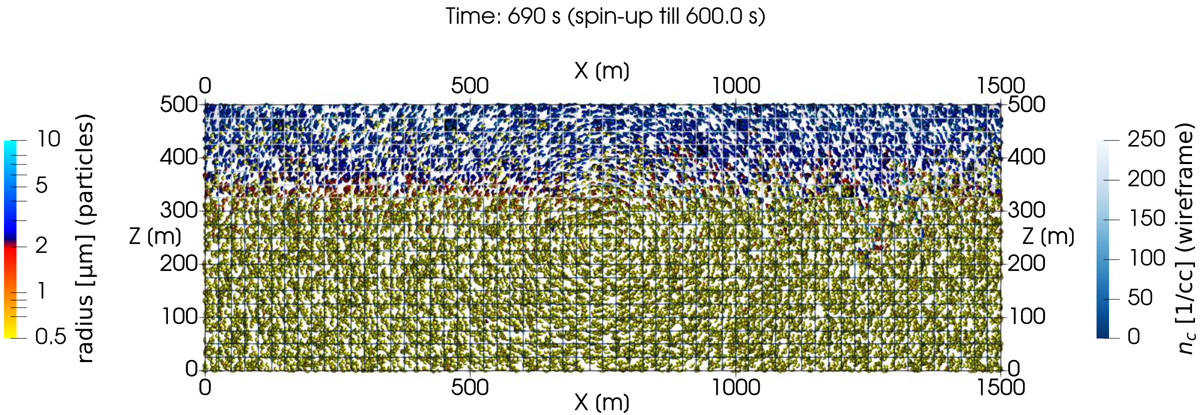

16+16 super-particles/cell for INP-rich + INP-free particles
$N_{aer} = 300/cc$ (two-mode lognormal) $N_{INP} = 150/L$ (lognormal, $D_g = 0.74$ μm, $\sigma_g = 2.55$)
spin-up = freezing off; subsequently frozen particles act as tracers

particle-based μ-physics + prescribed-flow test

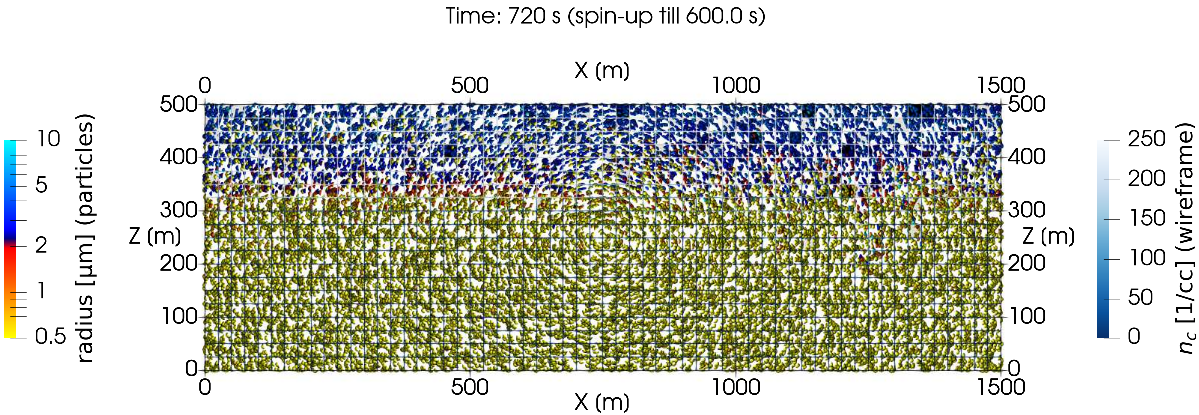

16+16 super-particles/cell for INP-rich + INP-free particles

$N_{aer} = 300/cc$ (two-mode lognormal) $N_{INP} = 150/L$ (lognormal, $D_g = 0.74$ μm, $\sigma_g = 2.55$)

spin-up = freezing off; subsequently frozen particles act as tracers

particle-based μ-physics + prescribed-flow test

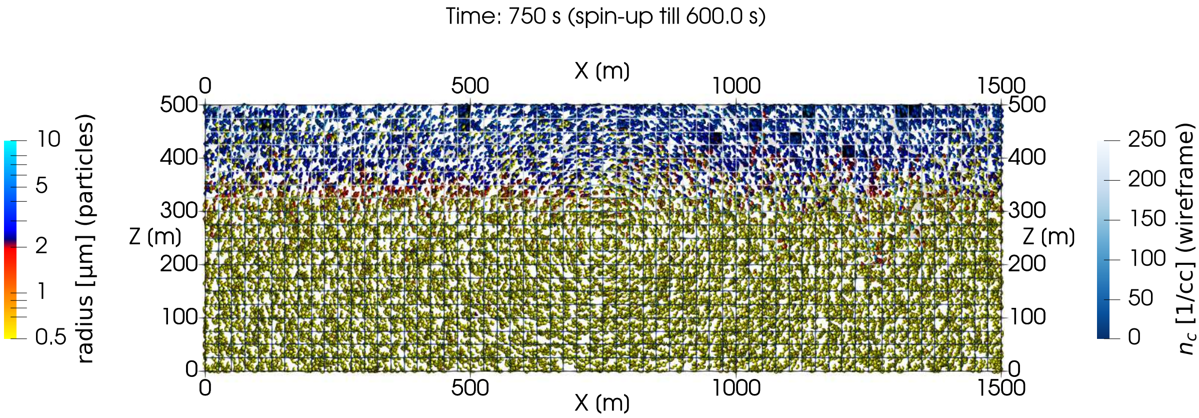

16+16 super-particles/cell for INP-rich + INP-free particles

$N_{aer} = 300/cc$ (two-mode lognormal) $N_{INP} = 150/L$ (lognormal, $D_g = 0.74$ μm, $\sigma_g = 2.55$)

spin-up = freezing off; subsequently frozen particles act as tracers

particle-based μ-physics + prescribed-flow test

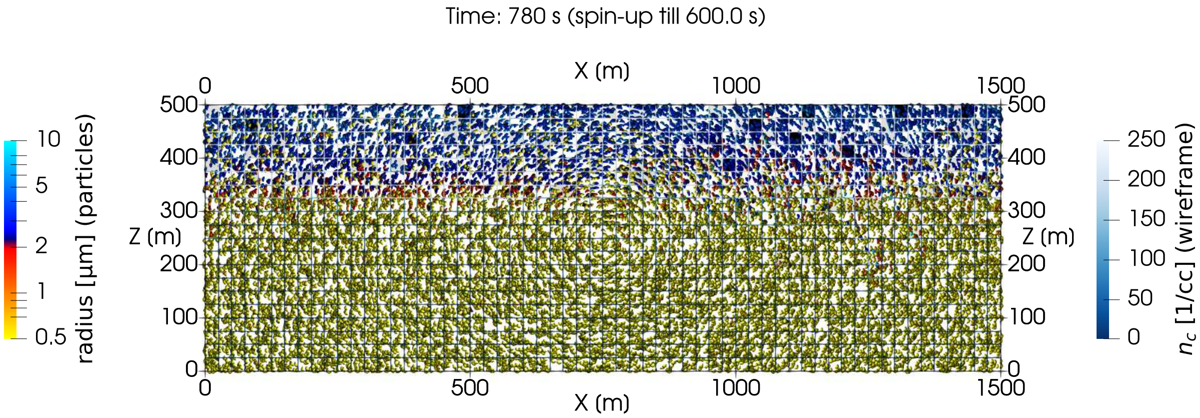

16+16 super-particles/cell for INP-rich + INP-free particles

$N_{aer} = 300/cc$ (two-mode lognormal) $N_{INP} = 150/L$ (lognormal, $D_g = 0.74$ μm, $\sigma_g = 2.55$)

spin-up = freezing off; subsequently frozen particles act as tracers

particle-based μ-physics + prescribed-flow test

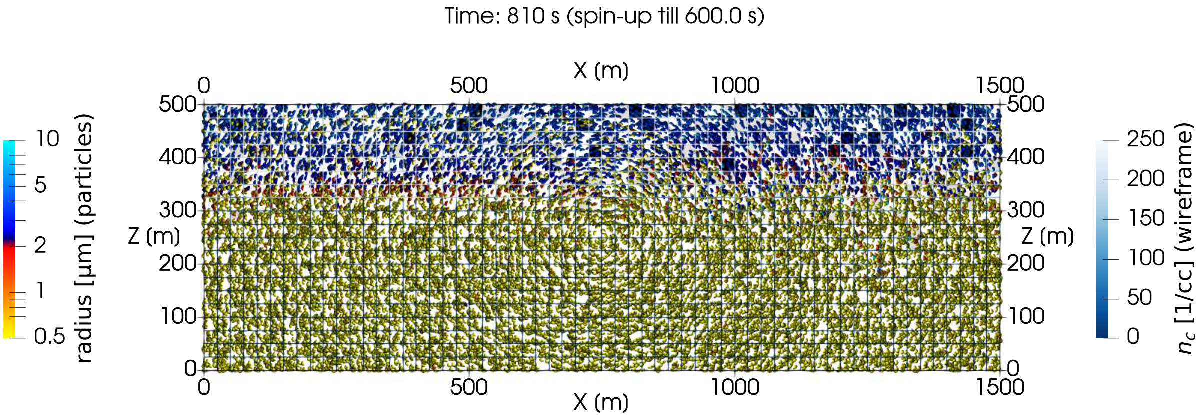

16+16 super-particles/cell for INP-rich + INP-free particles

$N_{aer} = 300/cc$ (two-mode lognormal) $N_{INP} = 150/L$ (lognormal, $D_g = 0.74$ μm, $\sigma_g = 2.55$)

spin-up = freezing off; subsequently frozen particles act as tracers

particle-based μ-physics + prescribed-flow test

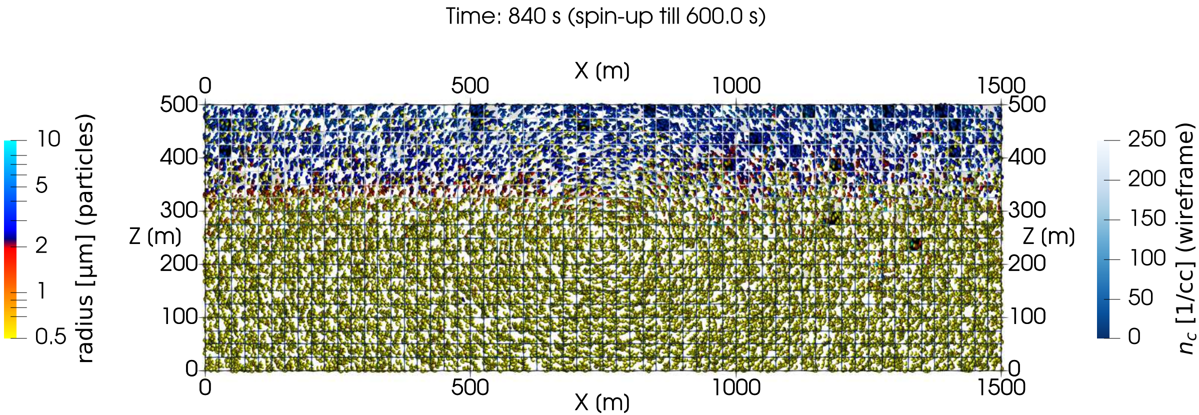

16+16 super-particles/cell for INP-rich + INP-free particles
$N_{aer} = 300/cc$ (two-mode lognormal) $N_{INP} = 150/L$ (lognormal, $D_g = 0.74$ μm, $\sigma_g = 2.55$)
spin-up = freezing off; subsequently frozen particles act as tracers

particle-based μ-physics + prescribed-flow test

Time: 870 s (spin-up till 600.0 s)

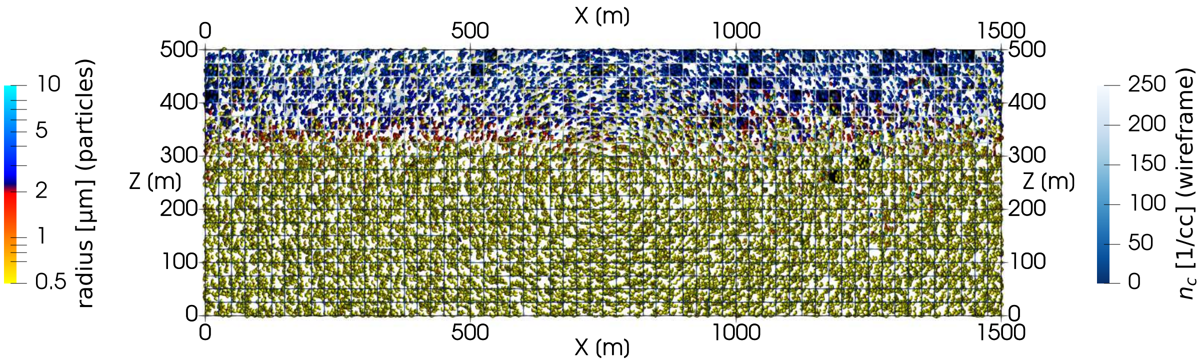

16+16 super-particles/cell for INP-rich + INP-free particles

$N_{aer} = 300/cc$ (two-mode lognormal) $N_{INP} = 150/L$ (lognormal, $D_g = 0.74$ μm, $\sigma_g = 2.55$)

spin-up = freezing off; subsequently frozen particles act as tracers

particle-based μ-physics + prescribed-flow test

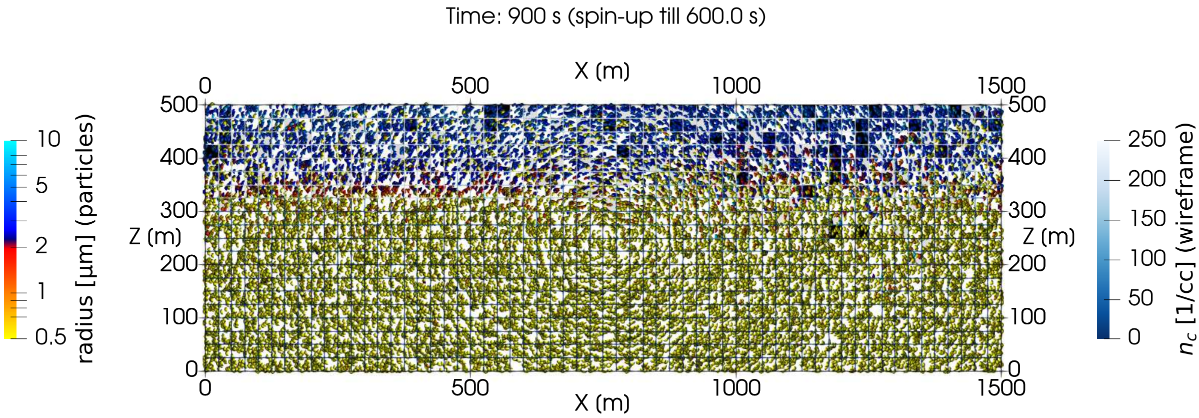

16+16 super-particles/cell for INP-rich + INP-free particles

$N_{\rm aer} = 300/cc$ (two-mode lognormal) $N_{\rm INP} = 150/L$ (lognormal, $D_g = 0.74$ μm, $\sigma_g = 2.55$)

spin-up = freezing off; subsequently frozen particles act as tracers

particle-based μ-physics + prescribed-flow test

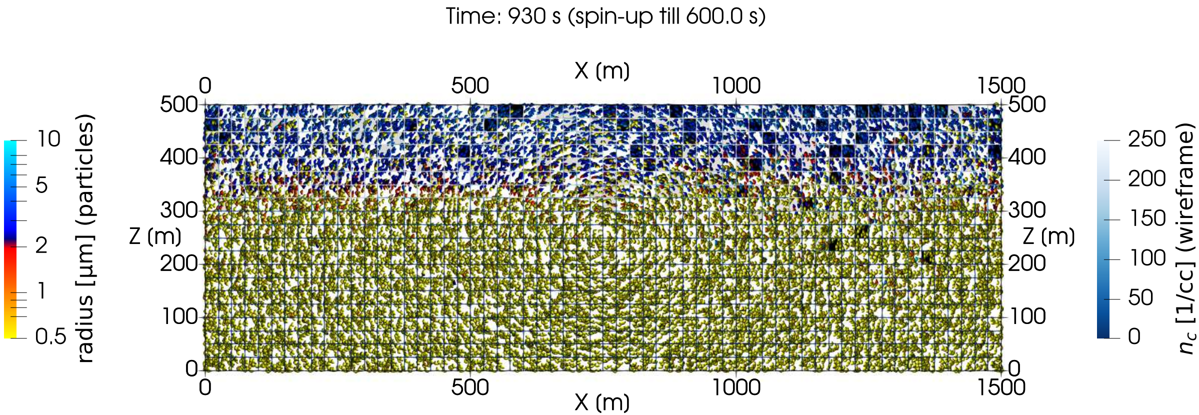

16+16 super-particles/cell for INP-rich + INP-free particles

$N_{aer} = 300/cc$ (two-mode lognormal) $N_{INP} = 150/L$ (lognormal, $D_g = 0.74$ μm, $\sigma_g = 2.55$)

spin-up = freezing off; subsequently frozen particles act as tracers

particle-based μ-physics + prescribed-flow test

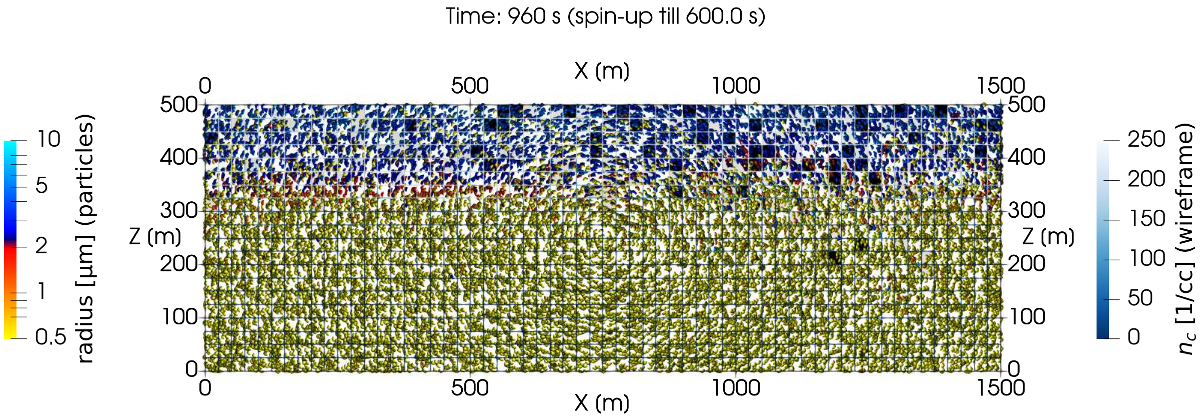

16+16 super-particles/cell for INP-rich + INP-free particles

$N_{\text{aer}} = 300/cc$ (two-mode lognormal) $N_{\text{INP}} = 150/L$ (lognormal, $D_g = 0.74$ μm, $\sigma_g = 2.55$)

spin-up = freezing off; subsequently frozen particles act as tracers

particle-based μ-physics + prescribed-flow test

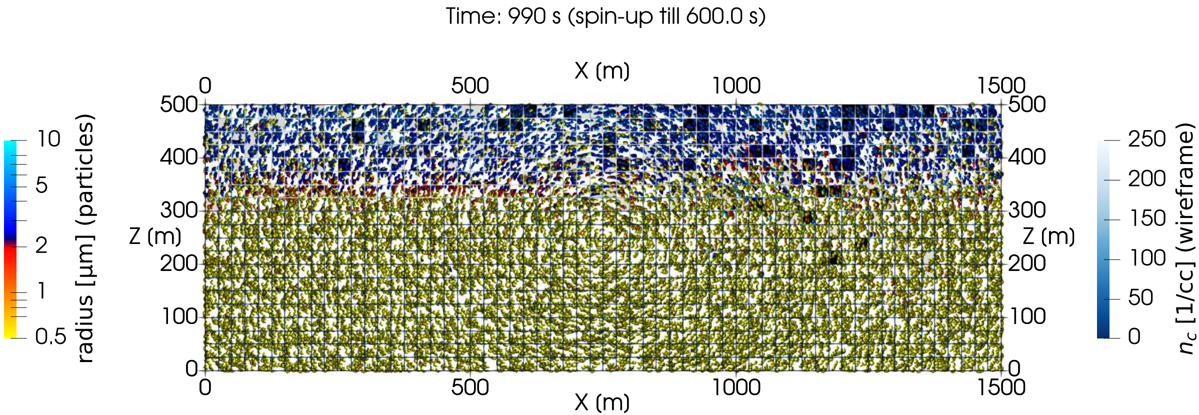

16+16 super-particles/cell for INP-rich + INP-free particles

$N_{\text{aer}} = 300/cc$ (two-mode lognormal) $N_{\text{INP}} = 150/L$ (lognormal, $D_g = 0.74$ μm, $\sigma_g = 2.55$)

spin-up = freezing off; subsequently frozen particles act as tracers

particle-based μ-physics + prescribed-flow test

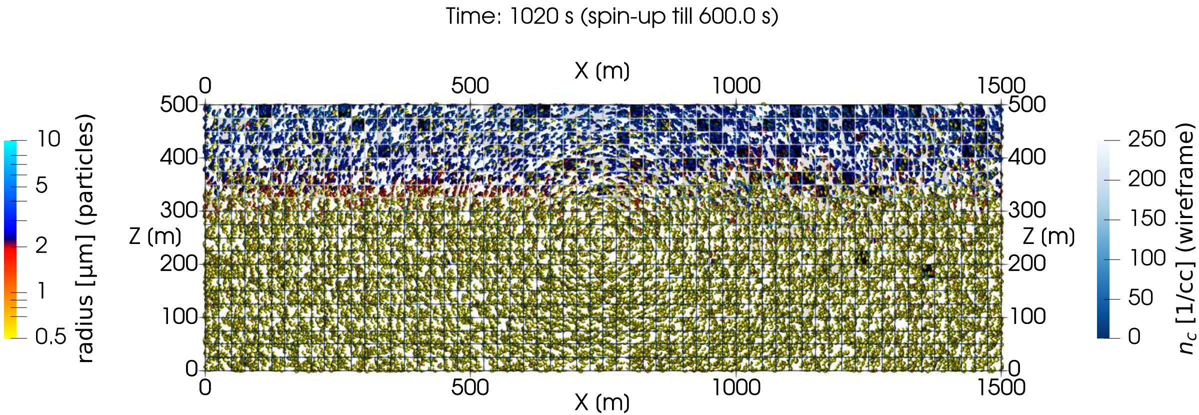

16+16 super-particles/cell for INP-rich + INP-free particles

$N_{aer} = 300/cc$ (two-mode lognormal) $N_{INP} = 150/L$ (lognormal, $D_g = 0.74$ μm, $\sigma_g = 2.55$)

spin-up = freezing off; subsequently frozen particles act as tracers

particle-based μ-physics + prescribed-flow test

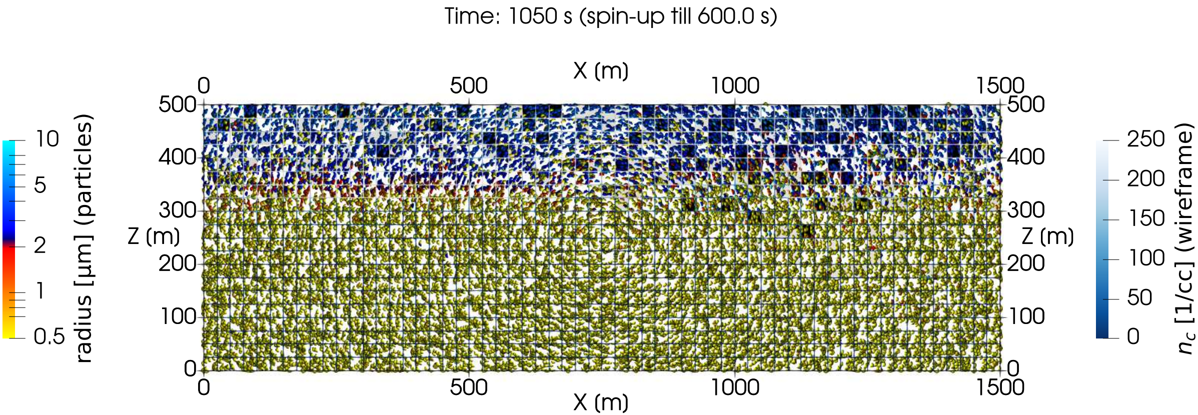

16+16 super-particles/cell for INP-rich + INP-free particles

$N_{aer} = 300/cc$ (two-mode lognormal) $N_{INP} = 150/L$ (lognormal, $D_g = 0.74$ μm, $\sigma_g = 2.55$)

spin-up = freezing off; subsequently frozen particles act as tracers

particle-based μ-physics + prescribed-flow test

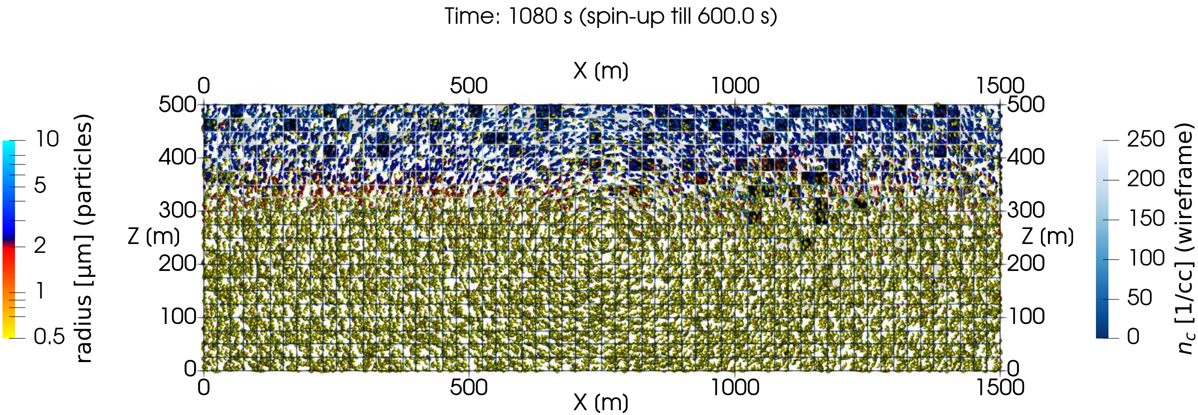

16+16 super-particles/cell for INP-rich + INP-free particles

$N_{aer} = 300/cc$ (two-mode lognormal) $N_{INP} = 150/L$ (lognormal, $D_g = 0.74$ μm, $\sigma_g = 2.55$)

spin-up = freezing off; subsequently frozen particles act as tracers

particle-based μ-physics + prescribed-flow test

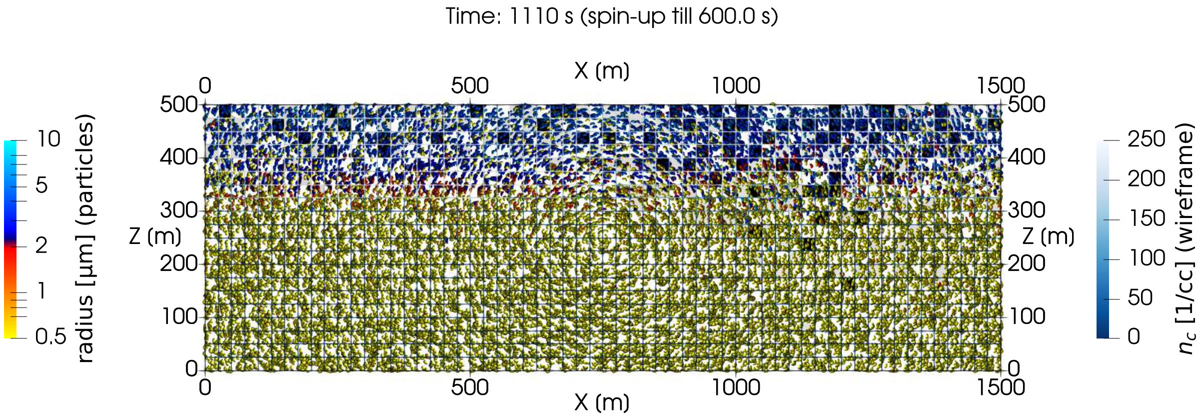

16+16 super-particles/cell for INP-rich + INP-free particles

$N_{\text{aer}} = 300/cc$ (two-mode lognormal) $N_{\text{INP}} = 150/L$ (lognormal, $D_g = 0.74$ μm, $\sigma_g = 2.55$)

spin-up = freezing off; subsequently frozen particles act as tracers

particle-based μ-physics + prescribed-flow test

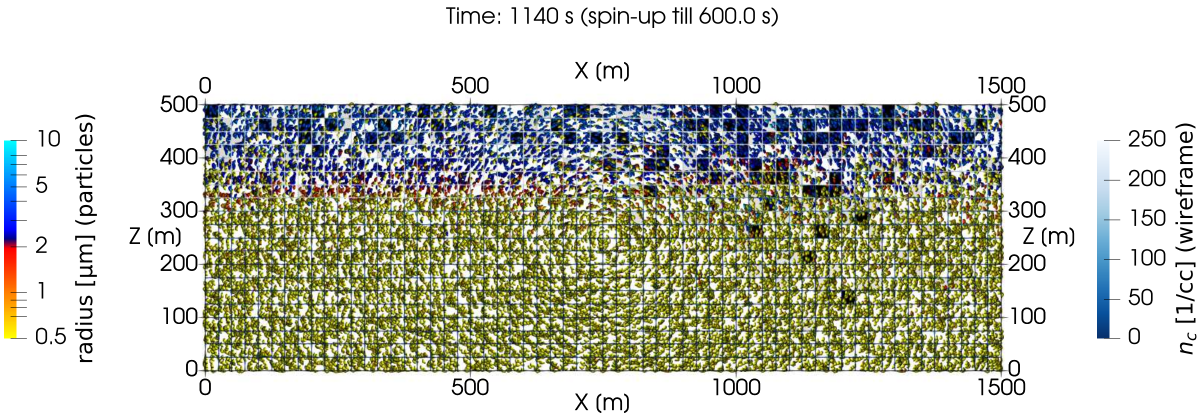

16+16 super-particles/cell for INP-rich + INP-free particles

$N_{aer} = 300/cc$ (two-mode lognormal) $N_{INP} = 150/L$ (lognormal, $D_g = 0.74$ μm, $\sigma_g = 2.55$)

spin-up = freezing off; subsequently frozen particles act as tracers

particle-based μ-physics + prescribed-flow test

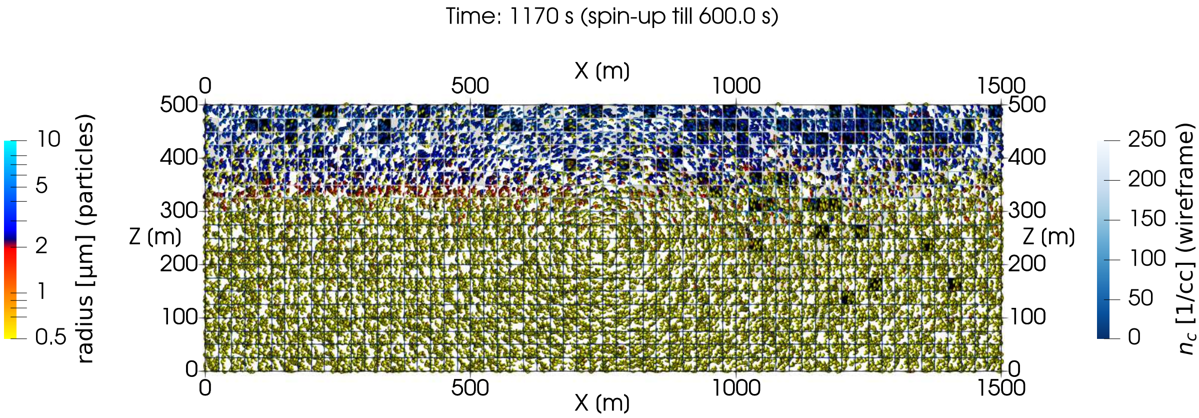

16+16 super-particles/cell for INP-rich + INP-free particles

$N_{aer} = 300/cc$ (two-mode lognormal) $N_{INP} = 150/L$ (lognormal, $D_g = 0.74$ μm, $\sigma_g = 2.55$)

spin-up = freezing off; subsequently frozen particles act as tracers

particle-based μ-physics + prescribed-flow test

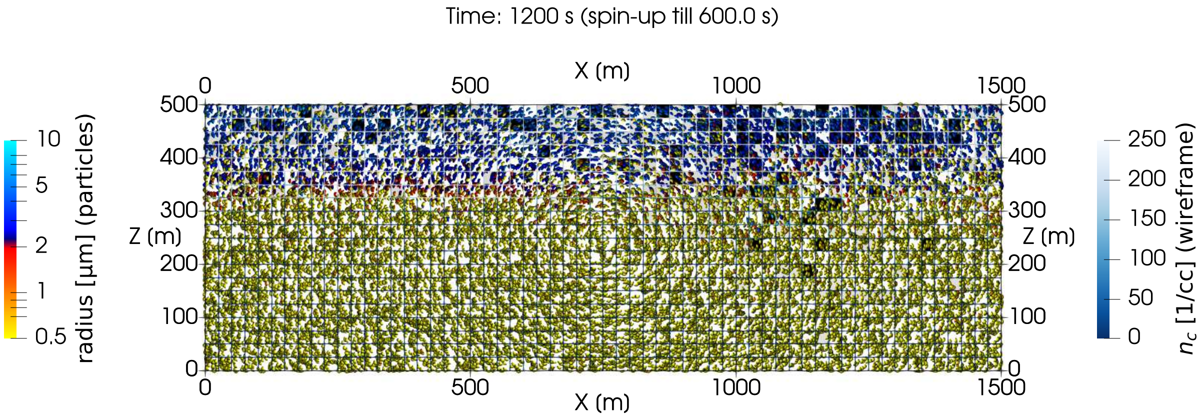

16+16 super-particles/cell for INP-rich + INP-free particles

$N_{aer} = 300/cc$ (two-mode lognormal) $N_{INP} = 150/L$ (lognormal, $D_g = 0.74$ μm, $\sigma_g = 2.55$)

spin-up = freezing off; subsequently frozen particles act as tracers

testing three flow regimes and two immersion freezing representations

$w_{max} \approx 1/3$ m/s

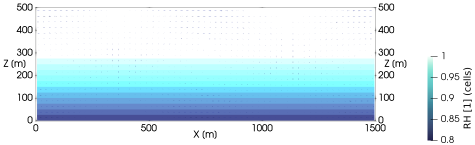

$w_{max} \approx 1$ m/s

$w_{max} \approx 3$ m/s

testing three flow regimes and two immersion freezing representations

$w_{max} \approx 1/3$ m/s

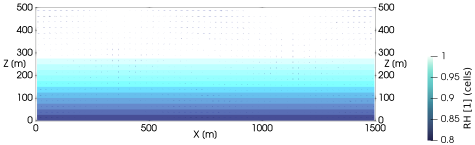

$w_{max} \approx 1$ m/s

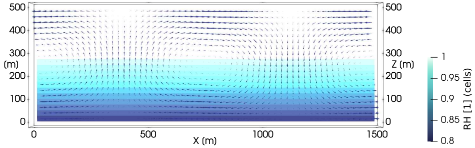

$w_{max} \approx 3$ m/s

testing three flow regimes and two immersion freezing representations

$w_{max} \approx 1/3$ m/s

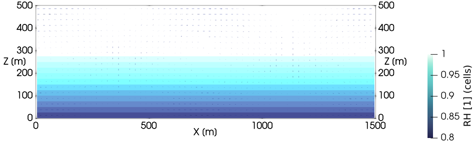

$w_{max} \approx 1$ m/s

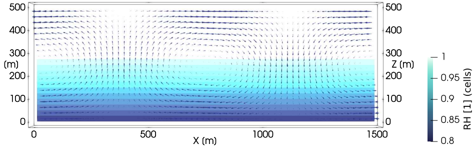

$w_{max} \approx 3$ m/s

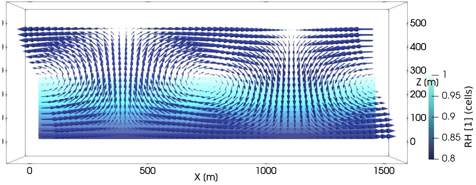

testing three flow regimes and two immersion freezing representations

$w_{max} \approx 1/3$ m/s

$w_{max} \approx 1$ m/s

$w_{max} \approx 3$ m/s

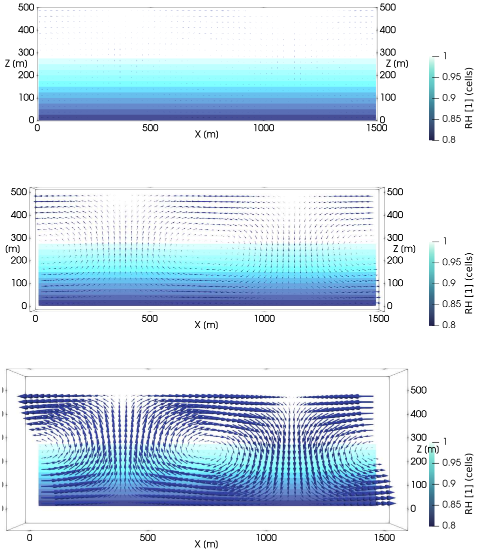

singular (INAS)

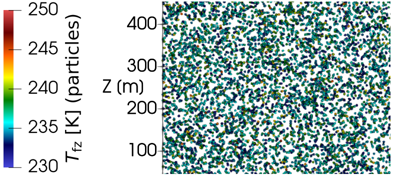

time-dependent (J_{het})

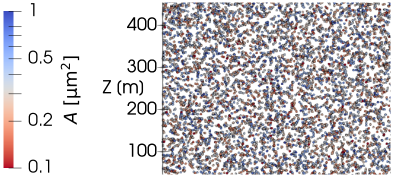

testing three flow regimes and two immersion freezing representations

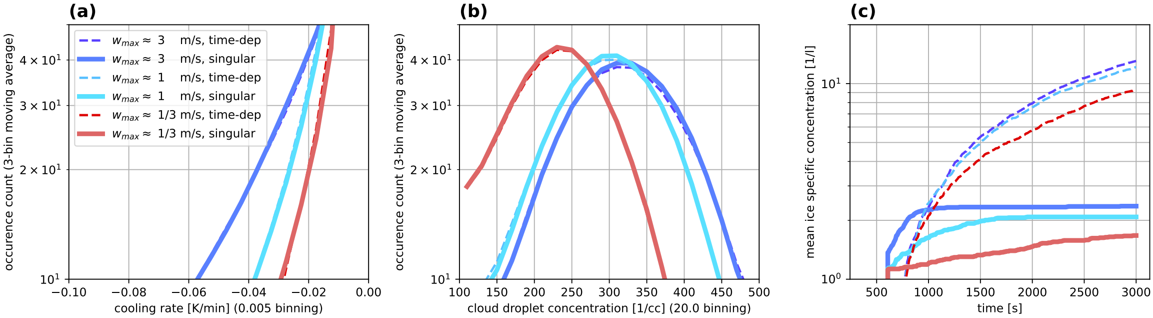

- range of cooling rates in simple flow (far from $c \sim 1$ K/min for AIDA as in Niemand et al. 2012)

testing three flow regimes and two immersion freezing representations

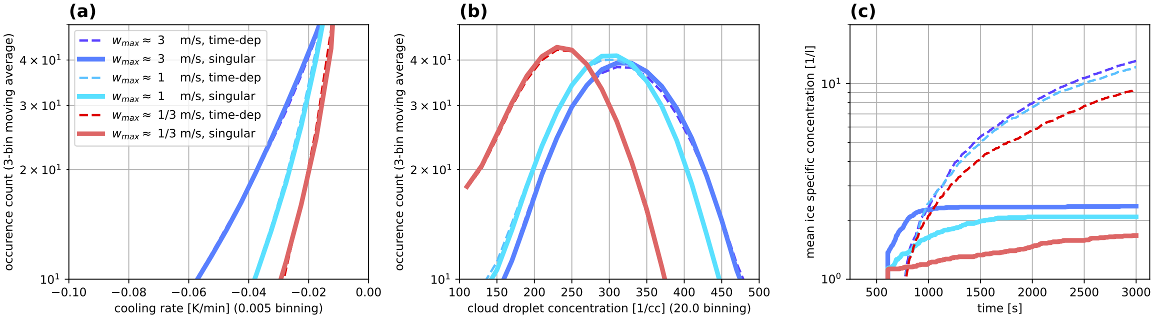

- range of cooling rates in simple flow (far from $c \sim 1$ K/min for AIDA as in Niemand et al. 2012)
- singular vs. time-dependent markedly different (consistent with box model for $c \ll 1K/min$)

testing three flow regimes and two immersion freezing representations

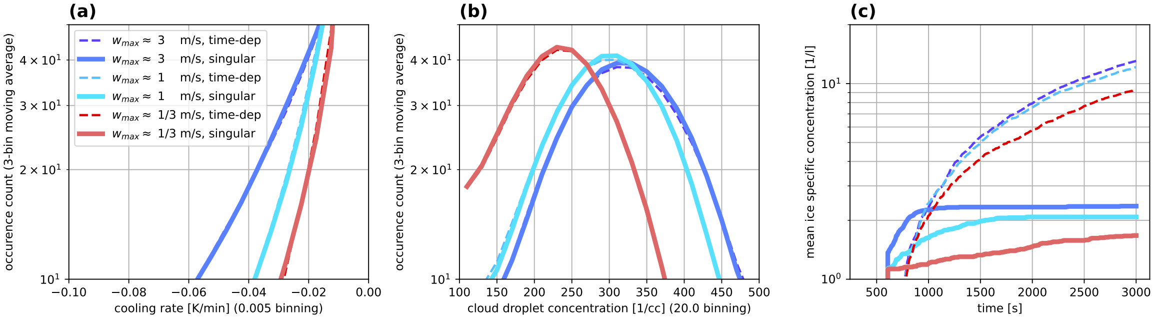

- range of cooling rates in simple flow (far from $c \sim 1$ K/min for AIDA as in Niemand et al. 2012)
- singular vs. time-dependent markedly different (consistent with box model for $c \ll 1K/min$)
- CPU time trade off: time dependent ca. 3-4 times costlier

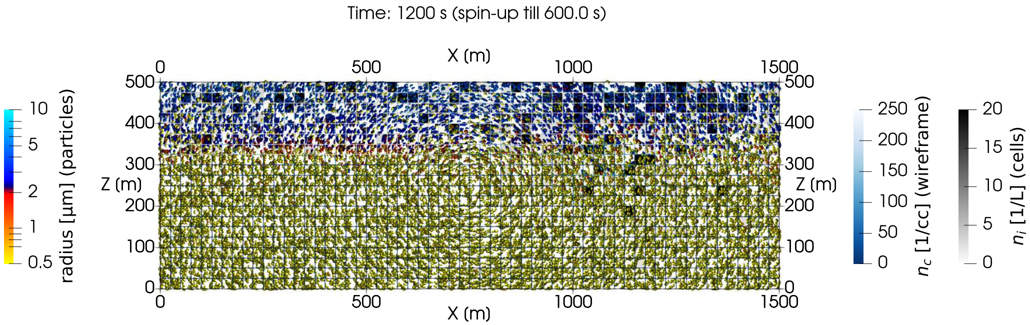

key messages:

– emergence of comprehensive mixed-phase particle-based aerosol/cloud μ-physics models

– cooling rate embedded in INAS fits ⇝ limited robustness to different flow regimes

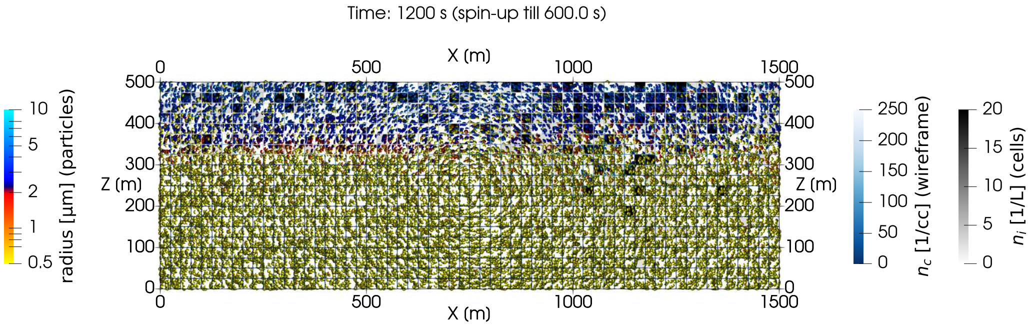

key messages:

– emergence of comprehensive mixed-phase particle-based aerosol/cloud μ-physics models

– cooling rate embedded in INAS fits ⇝ limited robustness to different flow regimes

ASR Atmospheric System Research DOE ASR grant no. DE-SC0021034

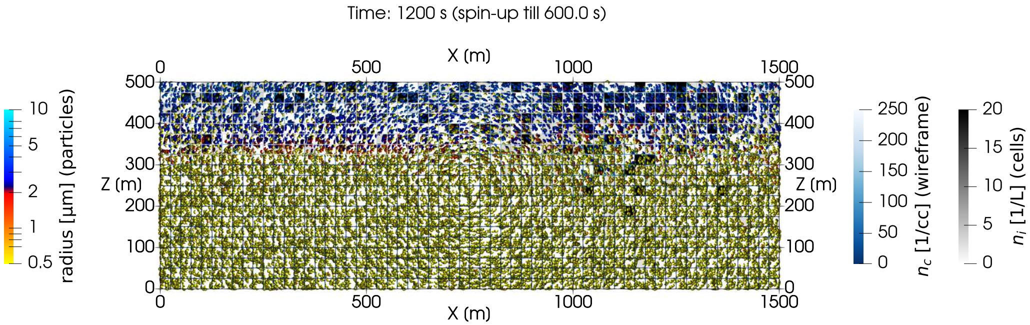

key messages:

– emergence of comprehensive mixed-phase particle-based aerosol/cloud μ-physics models

– cooling rate embedded in INAS fits ⇝ limited robustness to different flow regimes

ASR Atmospheric System Research

DOE ASR grant no. DE-SC0021034

project hosted at: ILLINOIS

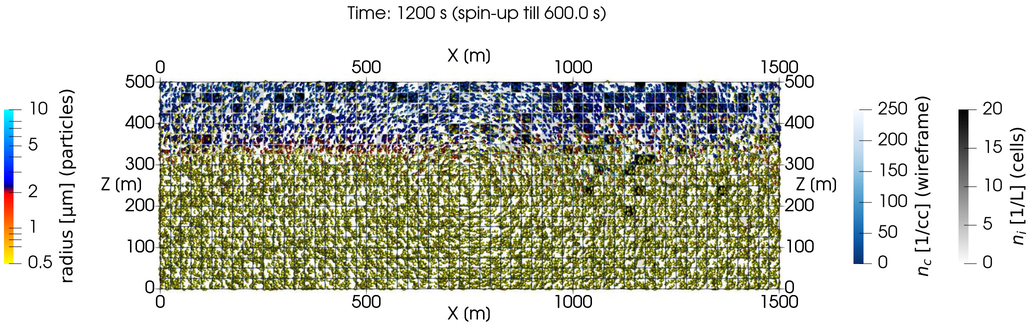

key messages:

– emergence of comprehensive mixed-phase particle-based aerosol/cloud μ-physics models

– cooling rate embedded in INAS fits ⇝ limited robustness to different flow regimes

ASR Atmospheric System Research DOE ASR grant no. DE-SC0021034

project hosted at: ILLINOIS

open python code: /atmos-cloud-sim-uj

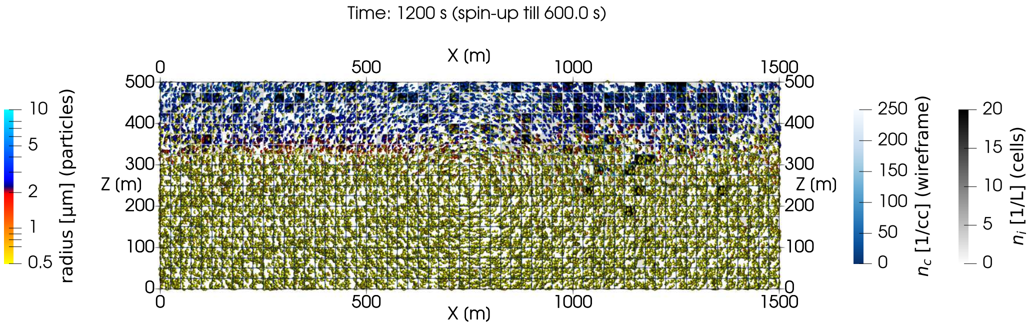

key messages:

– emergence of comprehensive mixed-phase particle-based aerosol/cloud μ-physics models

– cooling rate embedded in INAS fits ⇝ limited robustness to different flow regimes

ASR Atmospheric System Research DOE ASR grant no. DE-SC0021034

project hosted at: ILLINOIS

open python code: /atmos-cloud-sim-uj

Thank you for your attention!

https://annual.ametsoc.org/index.cfm/2023/program-events/call-for-papers/

AMS 2023 — 103rd ANNUAL MEETING — JANUARY 8-12 — DENVER & ONLINE — AMERICAN METEOROLOGICAL SOCIETY

15th Symposium on Aerosol–Cloud–Climate Interactions

The 15th Symposium on Aerosol–Cloud–Climate Interactions is sponsored by the American Meteorological Society and organized by the AMS Committee on Atmospheric Chemistry.

Call for Papers

Papers for the 15th Symposium on Aerosol–Cloud–Climate Interactions are solicited on the following:

- Advances in observational and modeling studies of mineral dust in the Earth system;
- Aerosol-Cloud Interactions in Deep Convective Clouds;
- Aerosol-Cloud interactions over the North Atlantic Ocean: insights from recent field campaigns;
- Aerosol-climate interactions from regional to global scale;
- Aerosol-cloud interactions in mixed-phase clouds;
- Aerosol-radiation interactions;
- Atmospheric ice-nucleating particles and ice formation processes in clouds;
- Challenges and progress in understanding, simulating and forecasting fog;
- Measurement and modeling of atmospheric cloud condensation nuclei and related chemistry;
- Mesoscale cloud organization and transition: the role of meteorology and aerosols;
- Probabilistic Particle-Based Methods in Aerosol-Cloud Microphysics Modeling.

Abstract Information

Abstracts are due by **24 August 2022 at 11:59 PM EDT**

SUBMIT ABSTRACT

Abstract Fee and Author Instructions